博士論文

Late Cornified Envelope Group I, a Novel Target of p53, Regulates PRMT5 Activity.

（新規 p53 標的遺伝子である Late Cornified Envelope Group I は PRMT5 の活性を調節する）

トウ　シン チュウ

鄧　振　忠

Deng, Zhenzhong

Late Cornified Envelope Group I, a Novel Target of p53, Regulates PRMT5 Activity.

（新規 p53 標的遺伝子である Late Cornified Envelope Group I は PRMT5 の活性を調節する）

所属　　東京大学大学院医学系研究科　病因・病理　専攻

指導教員　　古川　洋一　教授

申請者　　Deng,　Zhenzhong

トウ　シンチュウ

鄧　　振　忠

Table of Contents

Abstract

TP53 is one of the most important tumor suppressor genes involved in human carcinogenesis. Although downstream targets of p53 and their biological functions in cancer cells have been extensively investigated, it is still far from the full understanding. Here, I demonstrate that Late Cornified Envelope Group I (LCE1) genes including *LCE1A*, *LCE1B*, *LCE1C*, *LCE1E* and *LCE1F*, which are located in the LCE gene clusters encoding multiple well-conserved stratum-corneum proteins, are novel downstream targets of p53. Exogenous p53 overexpression using an adenoviral vector system significantly enhanced the expression of *LCE1* cluster genes. I also observed induction of LCE1 expression by DNA damage, which was caused by treatment with Adriamycin or ultra-violet irradiation (UVR) in a wild-type p53 dependent manner. Concordantly, the induction of *LCE1* by DNA damage was significantly attenuated by the knockdown of p53. Among predicted p53-binding sites within the *LCE1* gene cluster, I confirmed one site to be a p53-enhancer sequence by reporter assays. Furthermore, I found that LCE1F, a member of LCE1 family, interacts with protein arginine methyltransferase 5 (PRMT5). Knockdown of LCE1 by specific siRNAs significantly increased the symmetric di-methylation of histone H3 arginine 8, a substrate of PRMT5, and overexpression of LCE1F remarkably decreased its methylation level. My data

suggest that LCE1 family members are novel p53 downstream genes and that they might modulate the activity of PRMT5 through the binding with PRMT5.

Abbreviations

Ad	Adenovirus
aDMA	asymmetric ω-$N^{'G}$, $N^{'G}$-Di-Methylation of Arginine
ADR	Adriamycin
B2M	β2-Microglobulin
BRG1	Brahma-related gene 1
ChIP	Chromatin Immunoprecipitation
DAPI	4',6-diamidino-2-phenylindole
EGFP	Enhanced Green Fluorescent Protein
EST	Expressed Sequence Tag
FLAG	A FLAG tag consisting of eight amino acids DYKDDDDK
GST	Glutathione *S*-transferase, 211 amino acid protein (26kDa)
H3R8me2s	Symmetrical Di-Methylation of Histone 3 Arginine 8
HA	human influenza Hemagglutinin consisting of nine amino acids YPYDVPDYA
hBRM	human Brahma
HEK293T	Human Embryonic Kidney cell 293 with T antigen
ICC	Immunocytochemistry

LCE1	Late Cornified Envelope Group I
LC-MS/MS	Liquid Chromatography-tandem Mass Spectrometry
MOI	Multiplicity of Infection
MMA	ω-$N^{'G}$-Mono-Methyl Arginine
mut	mutant
p53BS	p53-binding sites
pRL-CMV	Plasmid containing CMV (CytoMegaloVirus) enhancer to highly express the Renilla luciferase
PRMT5	Protein arginine methyltransferase 5
qPCR	quantitative real-time PCR (Polymerase Chain Reaction)
RB	Retinoblastoma
SAM	S-adenosylmethionine
sDMA	symmetric ω-$N^{'G}$, $N^{'G}$-Di-Methylation of Arginine
SDS-PAGE	Sodium Dodecyl Sulfate PolyAcrylamide Gel Electrophoresis
siRNAs	small interfering RNAs
UVR	Ultra-Violet irradiation
wt	wild-type

Introduction

TP53 is the most frequently mutated tumor suppressor gene involved in human cancer [1, 2]. Particularly in human ovarian, colorectal, head and neck, and esophagus cancers, somatic mutation of *TP53* was found to be over 40% (Figure 1).

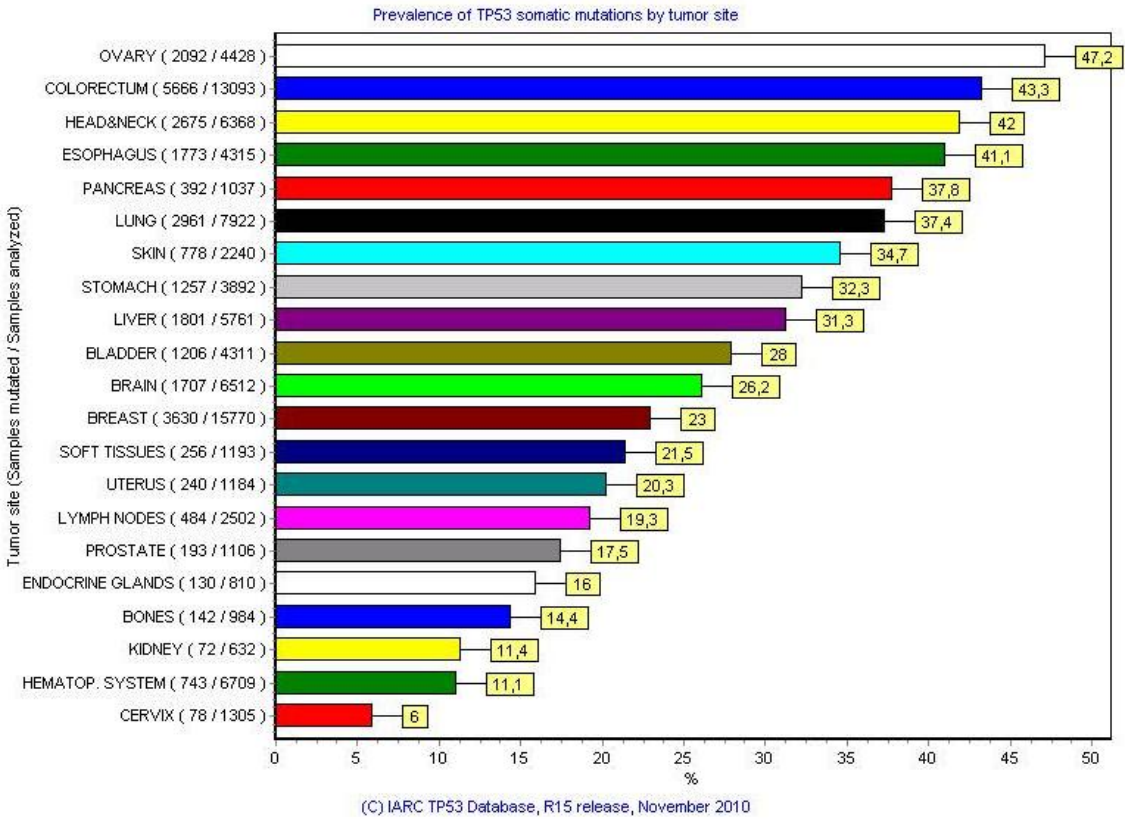

Figure 1. Prevalence of *TP53* mutation by tumor sites (R15 release November 2010) from IARC TP53 database at http://p53.iarc.fr/**.**

Its tetramer protein product can activate the transcription of a number of target downstream genes and mediate a variety of biological functions through the transcriptional regulation of those targets [3]. To elucidate the critical roles of p53 in human carcinogenesis, we and others have been attempted to identify p53-target genes

through multiple approaches [4-7] (Figure 2). We have mainly applied the expression profile analysis after the exogenous introduction of wild-type p53 into cancer cells using the adenovirus vector system and identified more than fifty p53-downstream candidate genes [8]. Among them, other members in my laboratory earlier performed the functional analysis of more than a dozen of target genes including *p53R2*, *p53AIP1* and *p53RDL1* [4-7]. I here report characterization of the Late Cornified Envelope Group I (LCE1) family members as novel downstream targets of p53.

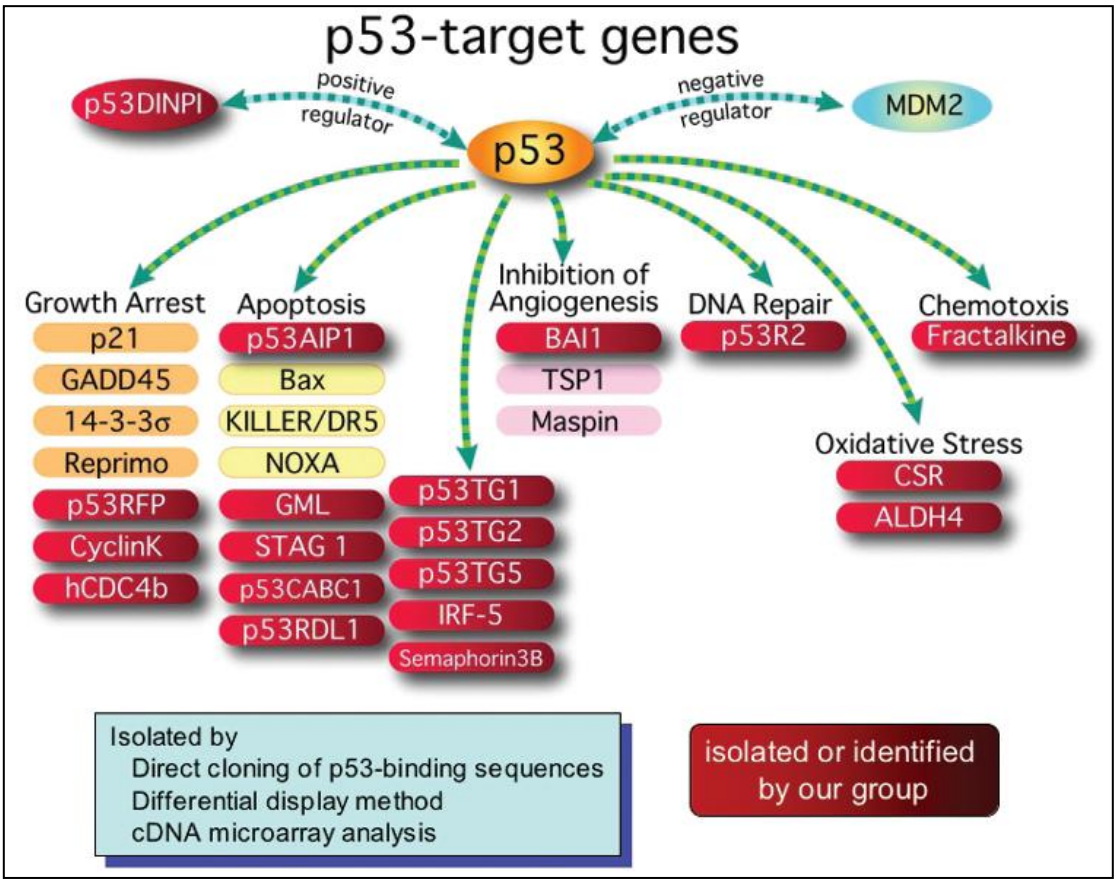

Figure 2. p53-target genes and their physiological roles. Classification of representative p53-target genes according to their biological function. Genes isolated in our group are highlighted in red color.

The *LCE* clusters contain multiple well-conserved genes encoding stratum-corneum proteins [9, 10]. Stratum-corneum is the outermost layer of the epidermis, consisting of dead cells (corneocytes). The integrity of the corneocytes depends on the outer cornified envelope and is essential for maintenance of barrier function. Thus, the stratum corneum provides the primary barrier against various environment stresses such as UV irradiation. [9-11]. The *LCE* clusters are located on chromosome 1q21 in a region called as the epidermal differentiation complex [12, 13] (Figure 3). This region is enriched for genes, which are expressed during epidermal differentiation, including *loricrin*, *involucrin*, *filagrin*, the small proline-rich protein genes, and the *LCE* genes [9, 14]. In mice, members in the Lce1 gene cluster are expressed in the relatively late stage of epithelial development and incorporated into the epidermal cornified envelope through cross-linking by transglutaminases [10, 15]. In addition, real-time qPCR analysis demonstrated that human *LCE1* and *LCE2* genes were primarily expressed in skin, whereas *LCE4* and *LCE5* gene expressions were undetectable in any human tissues examined [9]. In general, physiological functions of LCE proteins, especially their involvement in human cancer are still largely unknown.

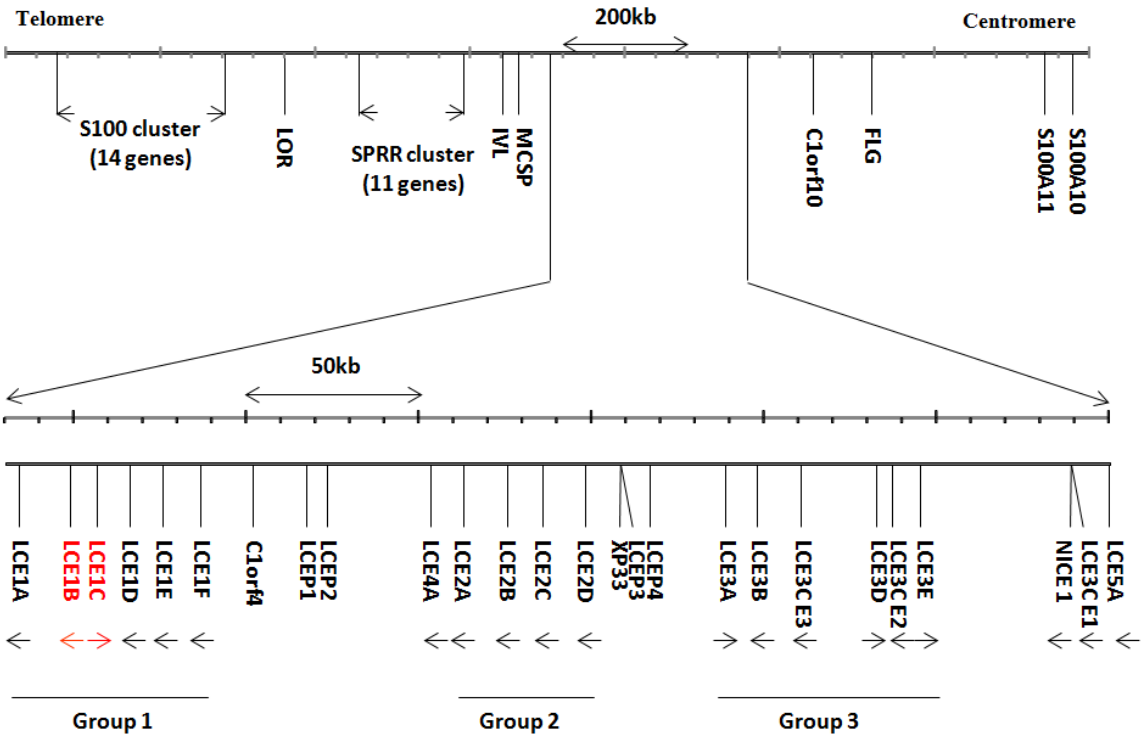

Figure 3. Schematic presentation of LCE gene clusters in human. Inset shows the LCE genes that cluster into three groups, LCE1, LCE2, and LCE3. Arrows indicate the direction of transcription. Adapted from [9].

Protein arginine methyltransferases (PRMTs) constitute of a large family of enzymes having the arginine methyltransferases activity responsible for catalyzing the formation of ω-$N^{'G}$-mono-methyl arginine (MMA), asymmetric ω-$N^{'G}$, $N^{'G}$-di-methyl arginine (aDMA) and symmetricω-$N^{'G}$, $N^{'G}$-di-methyl arginine (sDMA), in a

S-adenosylmethionine (SAM) dependent manner (Figure 4) [16, 17]. PRMT5 is one of the most well-characterized family members with sDMA activity and catalyzes formation of sDMA in proteins with a glycine and arginine-rich motif [18]. PRMT5 was reported to regulate various cellular functions including apoptosis, Golgi structure, pluripotency, cell growth and snRNP biosynthesis [19-22]. One important key marker of the PRMT5 activity is the symmetrical di-methylation of Histone 3 Arginine 8 (H3R8me2s) level. Through hypermethylation of histone H3R8 around the promoter regions, PRMT5 could cause the transcriptional silencing of cell cycle regulator genes [22-24]. Since overexpression of PRMT5 has been reported in various types of human cancer, including melanoma, leukemia, lymphoma, glioma, as well as ovarian, breast, prostate and lung cancers [17, 19, 22, 25-28], this enzyme is considered as a good molecular target for development of novel cancer therapy [17, 19, 22].

In the present study, I firstly demonstrate that LCE1 genes are novel targets of p53, and that LCE1F can interact with PRMT5. In addition, I found that LCE1 might modulate histone H3 methylation by PRMT5. This mechanism may be important for the interplay of two important cancer-related genes, p53 and PRMT5, and my findings could indicate a possible role of LCE1 in human carcinogenesis.

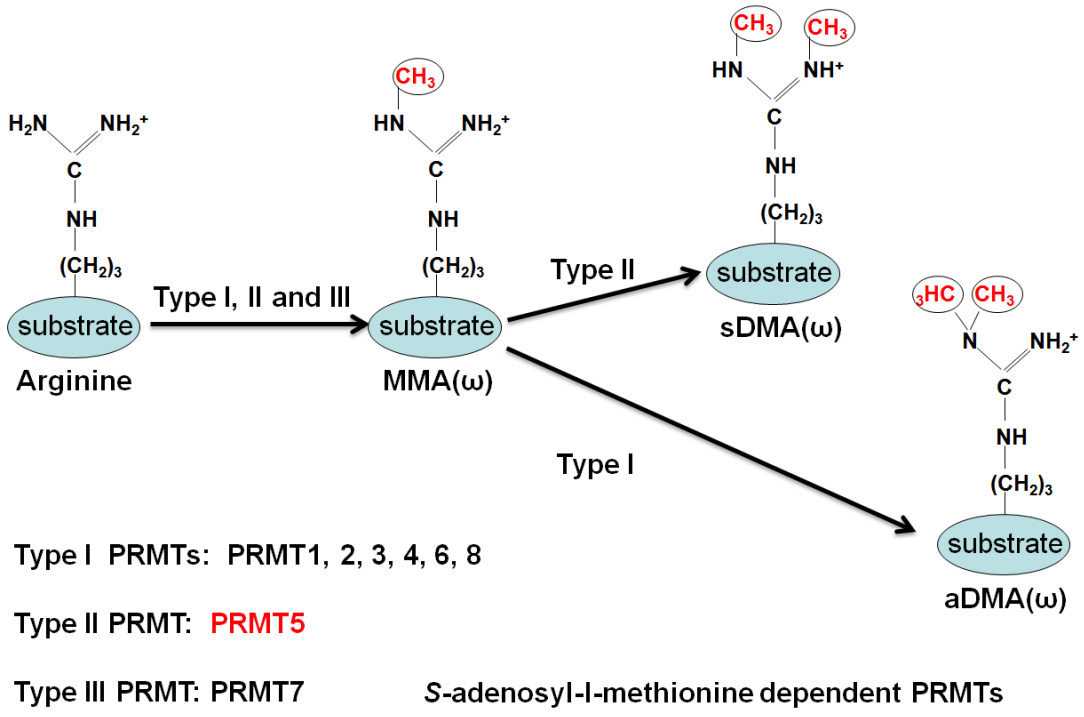

Figure 4. Classification and function of PRMT family members. The type I PRMTs can catalyze the substrate into ω-$N^{'G}$-mono-methyl arginine (MMA) as well as asymmetric ω-$N^{'G}$, $N^{'G}$-di-methyl arginine (aDMA), while the type II PRMTs can form MMA as well as symmetric ω-$N^{'G}$, $N^{'G}$-di-methyl arginine (sDMA). On certain circumstances, PRMT7 functions as a type III enzyme, which only generates MMA products. All types of PRMTs could generate MMA in *S*-adenosyl-l-methionine dependent manner. Adapted from [16, 17].

Materials and Methods

Microarray Analysis

Replication-deficient recombinant adenovirus designed to express wild-type p53 (Ad-p53) or LacZ (Ad-LacZ) was generated and purified, as previously described [4, 29]. Microarray analysis was carried out as previously described [1, 8, 29]. In brief, poly(A)+ RNAs were isolated from U373MG cells at different time points after infection with Ad-p53 or Ad-LacZ**.** Each RNA sample was labeled and hybridized to a microarray consisting of 36,864 genes or ESTs (http://www.ncbi.nlm.nih.gov/geo/index.cgi, Accession No. GSE14953).

Cell Culture and Transfection

Human cell lines, U373MG (glioblastoma), H1299 (lung carcinoma) and HEK293T, were purchased from American Type Culture Collection (ATCC, Manassas, VA). HCT116 $p53^{-/-}$ and HCT116 $p53^{+/+}$ cell lines were obtained from Dr. Bert Vogelstein (Johns Hopkins University, Baltimore, MD). U373MG glioblastoma cells and H1299 lung cancer cells were infected with Ad-p53 or Ad-LacZ at various multiplicity of infection (MOI) conditions and incubated at 37°C until the time of harvest. HEK293T cells were transfected with HA-Mock (empty vector of pCAGGSnHC) or HA-LCE1

expression plasmids (pCAGGSnHC-LCE1A, 1B, 1C, 1E and 1F) using FuGENE6. For protein-protein interaction experiments, HEK293T cells were transfected with HA-Mock or HA-LCE1F, and FLAG-Mock (empty vector of pCAGGSn3FC) or FLAG-PRMT5 (pCAGGSn3FC-PRMT5) using FuGENE6. To examine the co-localization, HCT116 $p53^{+/+}$ cells were transfected by HA-Mock or HA-LCE1F using FuGENE6. For the gene reporter assay, U373MG (mutated p53) and H1299 (p53 null) cells were transfected with reporter plasmids, and either a Mock empty vector of pcDNA3.1+ or a wild-type p53 expression pcDNA3.1+ vector in combination with a pRL-CMV vector using FuGENE6 [30, 31]. Small interfering RNAs (siRNAs) that were commercially synthesized by Sigma-Aldrich (St. Louis, MO), were transfected with Lipofectamine® RNAiMAX reagent (Life Technology, Carlsbad, CA). siRNA targeting p53 was used to be the positive control siRNA while siRNA of EGFP as negative control for the transfection of siRNA. Two siRNA oligonucleotides were designed to target the different coding sequence region of *PRMT5* specifically. Two siRNA oligonucleotides of *LCE1A-F* were designed to target the region commonly-conserved among *LCE1A-F*. Sequences of oligonucleotides are shown in Table 1. Western blot or quantitative real-time PCR was applied to validate the efficiency of overexpression or knockdown experiments.

Table 1. Oligonucleotides used for the preparation of siRNA.

Target Gene	siRNA	Oligonucleotide Sequence
si-p53	Sense	5’-GACUCCAGUGGUAAUCUACTT-3’
	Antisense	5’-GUAGAUUACCACUGGAGUCTT-3’
si-EGFP	Sense	5’-GCAGCACGACUUCUUCAAGTT-3’
	Antisense	5’-CUUGAAGAAGUCGUGCUGCTT-3’
si-LCE1#21	Sense	5’-UCCGGAGGCUGCUGUGGCUTT-3’
	Antisense	5’-AGCCACAGCAGCCUCCGGATT-3’
si-LCE1#24	Sense	5’-GGAGGCUGCUGUGGCUCCATT-3’
	Antisense	5’-UGGAGCCACAGCAGCCUCCTT-3’
si-PRMT5#1	Sense	5’-CACCUAAUGCCUAUGAACUTT-3’
	Antisense	5’-AGUUCAUAGGCAUUAGGUGTT-3’
si-PRMT5#2	Sense	5’-GCUCAUUUGCUGACAAUGATT-3’
	Antisense	5’-UCAUUGUCAGCAAAUGAGCTT-3’

DNA-damaging Treatments

Cells were seeded 24 hours before treatment. When cells reached at the 60–70% confluent, cells were incubated with 1 μg/ml of Adriamycin for 2 h followed by further incubation the drug-free medium. Then the cells were harvested at different time points as indicated in the figure legends. For UV irradiation experiments, the cells were washed twice with phosphate-buffered saline (PBS) and exposed to UV rays at different doses using XL-1500 Spectrolinker (Spectronics, New York, US) (peak emission, 254 nm). Cells were harvested 36 h after the UV irradiation.

Quantitative Real-time PCR

Total RNA was isolated from cultured cells using RNeasy mini-spin column kits (Qiagen, Hilden, Germany) according to the manufacturer's procedure. cDNAs were synthesized with the SuperScript Pre-amplification System (Life Technology). Quantitative real-time PCR was conducted using the SYBR Green I Master on the LightCycler 480 (Roche) according to the manufacturer's instructions. The primer sequences used in this manuscript are shown in Table 2. Primers for *LCE1A*, *LCE1C*, *LCE1E* and *LCE1F* were described previously [9], while primers for *LCE1B*, *LCE1D* *LCE3A*, *LCE3B*, *LCE3C*, *LCE4A*, *XP33* and *C1orf45* genes were designed by us. The specificity of all PCR products for *LCE1A*, *LCE1B*, *LCE1C*, *LCE1E*, *LCE1F*, *LCE3A*, *LCE3B*, *LCE3C*, *LCE4A*, *XP33* and *C1orf45* were confirmed by DNA sequencing. But I could not get a specific band of the *LCE1D* product with various primer sets for *LCE1D*. For graphic representation of transcript data, all expression of target genes was shown relative to the expression of a housekeeping gene, β2-microglobulin, in the same sample.

Table 2. Primers used for the quantitative real-time PCR.

Gene	Size	Direction	Sequence
LCE1A	132 bp	Forward	5'-TGCAAGAGTGGCTGAGATGC-3'
		Reverse	5'-AGACAACACAGTTGGTGTCAGG-3'
LCE1B	65 bp	Forward	5'-TCTTCTGTCTTGGAGTTCAGAGG-3'
		Reverse	5'-TGAGGTCATTAAATGGCTTGG-3'
LCE1C	73 bp	Forward	5'-GAATCCAGGACCGCAAACTG-3'
		Reverse	5'-TGGACCTGTGAGCCTCTCAG-3'
LCE1E	129 bp	Forward	5'-TGAATAGCTGAGAGGTTCCAGC-3'
		Reverse	5'-CAGCCATGGATCTGCAGAAG-3'
LCE1F	138 bp	Forward	5'-CTTGGGACTGACTGTGTTGC-3'
		Reverse	5'-AGGCGCACAGATGGAATCA-3'
LCE3A	83 bp	Forward	5'-CCTGAGTCACCACAGATGCC-3'
		Reverse	5'-CTTGCTGACCACTTCCCCTG-3'
LCE3B	211 bp	Forward	5'-CCCAAAGAGCTCAGCACAGT-3'
		Reverse	5'-TCCAGAGCCATAGCCACAGT-3'
LCE3C	62 bp	Forward	5'-GTGGCCCCAGTTCTGAAA-3'
		Reverse	5'-TTGATGGGACCTGAAGTGC-3'
LCE4A	89 bp	Forward	5'-CCACAGACACCATAGGTCCC-3'
		Reverse	5'-AGCCAGAACCCCCAGACT-3'
C1orf45	60 bp	Forward	5'-TCCCCAGGCCATACTTTAGA-3'
		Reverse	5'-AGAGTGGGGAAGAGTGAGCA-3'
XP33	72 bp	Forward	5'-TGTCTCAGAAGCAGCCATTG-3'
		Reverse	5'-CATCCAAACTTCAAGAGAGCAA-3'
β2M	86 bp	Forward	5'-TTCTGGCCTGGAGGCTATC-3'
		Reverse	5'-TCAGGAAATTTGACTTTCCATTC-3'

Prediction of Putative p53-binding Sites

DNA sequences of an entire genomic region of *LCE1* including 10 kb of 5' upstream sequence were downloaded from UCSC website (http://genome.ucsc.edu/) and the putative p53-binding sites were screened according to the following criteria; at least 80% matched with the 20 nucleotides of consensus sequence 5'-RRRCWWGYYY_RRRCWWGYYY-3' (R, purine; W, A or T; Y, pyrimidine).

Gene Reporter Assay

DNA fragments containing one of the 11 potential p53-binding sites in the *LCE1* gene cluster were amplified by PCR using KOD-Plus-DNA polymerase (Toyobo, Osaka, Japan). Subsequently, the PCR products were sub-cloned into the pGL3-promoter (pGL3-pro) vector. The primers for amplification are indicated in Table 3. For the preparation of plasmids containing mutant p53-binding site, the fourth and the fourteenth nucleotide 'C' and the seventh and the seventeenth nucleotide 'G' of the consensus p53-BS were substituted to 'T'. Namely, the consensus sequence of 5'-RRRCWWGYYY_RRRCWWGYYY-3' was changed to 5'-RRRTWWTYYY_RRRTWWTYYY-3' using the KOD-Plus- Mutagenesis Kit (Toyobo). Since a functional p53-binding site is known in the *Fas* promoter region, a

wild-type Fas promoter construct, pGL3-Fas, was used as a positive control. U373MG (mutated p53) and H1299 (p53 null) cells were plated in 12-well culture plates (5 x 10^4 cells per well) 24 hours before co-transfection of 125 ng of a reporter plasmid and either 125 ng of a Mock vector or a wild-type p53 expression vector in combination with 25 ng of a pRL-CMV vector. Cells were rinsed with PBS 36 hours after transfection and lysed in 250 μl of lysis buffer. Twenty and five μl of lysates from U373MG and H1299, respectively, were sequentially measured using the PGD-S Dual Luciferase assay system according to the manufacture's procedure (Toyo Ink, Tokyo, Japan). The firefly luciferase activity was normalized by the Renilla luciferase activity.

Table 3. Primers utilized for the reporter assay of p53BS

Fragment	Size	Direction	Sequence
p53BS1	335bp	Forward	5'-GTCATTCTGCTTGGCACAGA-3'
		Reverse	5'-AGCGTGCTAGTCCCTTCAAA-3'
p53BS2	313bp	Forward	5'-GAGGACTCCAGGAACCATGA-3'
		Reverse	5'-CAGGGCACACTTACCAGGAT-3'
p53BS3	408bp	Forward	5'-TGGCAGGTAAAGGGAGTGTC-3'
		Reverse	5'-CTGAAGTCTCCGCCAGTAGG-3'
p53BS4	414bp	Forward	5'-CTATCTAGCAGCAGGTGCCC-3'
		Reverse	5'-GAGAGGACTGCTCCACCCTA-3'
p53BS5	547bp	Forward	5'-CTGGGGTTTCATGGAAGGTA-3'
		Reverse	5'-TTCAAGGGCTTGACCAGTCT-3'
p53BS6	304bp	Forward	5'-AGCCCCAGCAACTATTCTCA-3'
		Reverse	5'-GGGATTTTCCCACTCCATTT-3'
p53BS7	220bp	Forward	5'-ATCCTGTCCTTTGGGCTCTT-3'
		Reverse	5'-ATCAAGGCAGGAGATGATGG-3'
p53BS7+8	785bp	Forward	5'-TTTTTCAGCAGACAAACACCTG-3'
		Reverse	5'-ATCAAGGCAGGAGATGATGG-3'
p53BS9	401bp	Forward	5'-TGCCACCATACCCAGCTAAT-3'
		Reverse	5'-GCCACCCTTATTGCCTTTTT-3'
p53BS10	437bp	Forward	5'-GCAAGATTGTGGGTTGTGTG-3'
		Reverse	5'-CTCTCCATCTTTGGGAGCTG-3'
p53BS11	338bp	Forward	5'-ACCTGTAGTCTCGGCCACTC-3'
		Reverse	5'-AGGAGGATTGCTTGAGTCCA-3'
p53BS11	338bp	Forward	5'-ACCTGTAGTCTCGGCCACTC-3'
		Reverse	5'-AGGAGGATTGCTTGAGTCCA-3'
p53BS2 mut	313bp	Forward	5'-TCTTATTCCCAGGCTCTGTCTCACCGC-3'
		Reverse	5'-GGAACTACCTCCCGACACCCACATAGG-3'
p53BS6 mut	304bp	Forward	5'-GGATCTTCCTTCTGACACCCACATGGG-3'
		Reverse	5'-TCTAATACCCAGGCCCTGTCTCACAGC-3'
p53BS7 mut	220bp	Forward	5'-TCTTATTCCCAGGCCCTGTCTCACTGC-3'
		Reverse	5'-GGAATTACCTCCTGACACCCACATAGGTCC-3'

Construction of Plasmids expressing PRMT5 and LCE1s

An entire coding sequence of PRMT5 was amplified using cDNA generated from mRNA of HEK293T cells and cloned into pCAGGSn3FC (PRMT5) vector containing three-tandem FLAG-epitope tags in the C-terminus of the cloning site [4, 29]. The entire coding sequences of *LCE1A-F* were amplified by the use of cDNA generated from HCT116 $p53^{+/+}$ cells treated with the 70 J/m^2 of UV-radiation. The PCR products of LCE1A, 1B, 1C, 1E and 1F were cloned into pCAGGSnHC vector containing an HA-epitope tag in the C-termius of the cloning site [4, 29]. Due to unknown reasons, I have been unsuccessful for the cloning of *LCE1D* cDNA. The DNA sequences of expression constructs for HA-LCE1 (pCAGGSnHC-LCE1A, 1B, 1C, 1E, and 1F) and FLAG-PRMT5 (pCAGGSn3FC-PRMT5) were confirmed by DNA sequencing using ABI PRISM® 3730XL Genetic Analyzer (Life Technologies).

Antibodies

The following primary antibodies were deployed; rabbit anti-HA (Y-11; Santa Cruz Biotechnology, Santa Cruz, CA; dilution used in WB: 1:1000), rabbit anti-PRMT5 (07-405; Millipore, Billerica, MA; dilution used for WB: 1:1000, and for immunocytochemistry: 1:400), rabbit anti-p53 (sc6243, Santa Cruz; dilution used in

WB: 1:1000), mouse anti-p53 (Ab-1, Calbiochem, San Diego, CA, dilution used in ChIP: 1:100), rabbit anti-H3R8me2s (ab130740, Abcam; dilution used in WB: 1:1000), mouse anti-α–Tubulin (clone DM1A, Millipore; dilution used in WB: 1:1000), rat anti-HA (3F10, Roche, dilution used in ICC: 1:800) and anti-FLAG (F7425, Sigma-Aldrich, dilution used in ICC: 1:1000).

Immunocytochemistry

Forty-eight hours after transfection with HA-Mock or HA-LCE1F into HEK293T or HCT116 $p53^{+/+}$ cells in 4-well chambers, the cells were fixed by 1.7% formaldehyde or 4% paraformaldehyde in PBS and permeabilized with 0.2% Triton X-100 in PBS. After covered with blocking solution (3% BSA in 0.2% Triton X-100) for 1 hour at room temperature, cells were incubated with a rat anti-HA antibody or a rabbit PRMT5 antibody overnight with humidified atmosphere at 4°C. Further, the cells were stained with fluorescence-conjugated secondary antibodies and then counterstained with the DAPI in VECTASHIELD® Mounting Media (HT1200, Vector Laboratory, Burlingame, CA).

Immunoprecipitation and Mass-Spectrometric Analysis

Forty-eight hours after transfection with HA-mock or HA-LCE1 expression plasmids (pCAGGSnHC-LCE1A, 1B, 1C, 1E and 1F), HEK293T cells were lysed in lysis buffer (50 mM Tris-HCl [pH 8.0], 0.4% NP-40, 150 mM NaCl) containing Protease Inhibitor Cocktail Set III (Calbiochem, San Diego, CA). Whole cell lysates were pre-cleared by incubation with normal mouse IgG (sc2025, Santa Cruz Biotechnology) and recombinant protein G-sepharose® 4B (Life Technology) at 4°C for 1 h, and subsequently incubated with anti-HA agarose (A2095, Sigma-Aldrich) overnight. The proteins were separated in Mini-PROTEAN 5–20% gradient SDS-PAGE precast gels (Bio-Rad Laboratories, Hercules, CA) and confirmed by HA antibody before the staining with the silver-staining kit (Life Technology). Four bands of 100 kDa, 70 kDa, 37 kDa, and 30 kDa were selected because they were detected in the precipitants of LCE1A, LCE1B, LCE1C, LCE1E, and LCE1F, but not in the precipitants of HA-Mock. Proteins were extracted from the four bands and analyzed by liquid chromatography-tandem mass spectrometry (LC-MS/MS) as previously described [32]. For the co-immunoprecipitation experiments, HEK293T cells were co-transfected with HA-LCE1F or HA-mock, and FLAG-PRMT5 or FLAG-Mock as a control. An HA pull-down experiment was carried out by the same method as

mentioned above. As for the pull-down experiment, whole cell lysates were pre-cleared by incubation with normal mouse IgG (sc2025, Santa Cruz Biotechnology) and recombinant protein G-sepharose®4B (Life Technology) at 4°C for 1 h, and subsequently incubated with mouse anti-FLAG M2 agarose (F3165, Sigma-Aldrich) overnight. Rat anti-HA (3F10, Roche) and rabbit anti-Flag (F7425, Sigma-Aldrich) antibodies were used for the western blot. For the histone methylation analysis, histones were extracted by the histone purification mini kit (40026, Active Motif, Carlsbad, CA) following the manufacture's procedure.

In Vitro Methyltransferase Assay

In vitro methyltransferase assays were performed as described previously [25]. Briefly, 1 μg of recombinant GST-LCE1F protein (H00353137-P01, Abnova, Taiwan) or 0.1 μg of synthetic LCE1F peptide (amino acid 76-94, CLSHHRRRRSHRHRPQSSD, purity> 95%) (Shanghai Hanhong Chemical Co. Ltd, Shanghai, China) was incubated with 1 μg of FALG-PRMT5 enzyme complex (Catalog #: 51045, Bpsbioscience, San Diego, CA) in 50 mM Tris–HCl (pH 8.8), 10 mM DTT, 10 mM $MgCl_2$, 1.0 μCi/ml S-adenosyl-L-[methyl-^{3}H]-methionine (Perkin Elmer, Waltham, MA) and Milli-Q water for 2 hour at 30°C. After boiling in sample buffer, the samples were subjected to

SDS-PAGE, and visualized by fluorography [25].

Chromatin Immunoprecipitation Assay (ChIP)

ChIP assays were performed using ChIP Assay kit (17-295; Millipore) according to the manufacture's protocol [33]. Briefly, HCT116 $p53^{+/+}$ cells were treated with 1 μg/ml of Adriamycin for 2 h, and the cells were cultured in the drug free-medium for 24 h. After fixation with formaldehyde, the cells were harvested and the complexes containing p53 were immnoprecipitated with an anti-p53 antibody (Ab-1, Calbiochem). After DNA fragments bound to p53 were eluted out, an aliquot was subjected to quantitative real-time PCR reactions. Protein A agarose/Salmon Sperm DNA (16-157; Millipore) was used as a negative control. Primers were designed to amplify the region containing the p53BS2 binding site, and the sequences of primers are shown in Table 4.

Table 4. Primers used for the ChIP assay of p53BS2

	Sequence	Length
Forward	5'-TGAAGGACGGTATATGCAGAACTGC-3'	25 bp
Reverse	5'-GGCCCTGAGCCCTTTTATTCTGTCC-3'	25 bp

Results

Identification of a Novel p53-downstream Target

In order to screen possible downstream genes that are regulated by p53, other members in our laboratory performed expression profile analysis of U373MG glioblastoma cells infected with wild-type p53 (Ad-p53) and those infected with LacZ (Ad-LacZ). Comparison between the profiles identified more than 50 genes that were likely to be transcriptionally activated by wild-type p53 [4, 29]. Among them, my colleagues and I confirmed that the transcriptional levels of Late Cornified Envelope Group 1B (LCE1B) and 1C (LCE1C) were elevated more than 7-fold higher in the cells infected with wild-type p53 than those with LacZ (Figure 5).

Spot	LMMID	Symbol	Gen Name	Set
H0967	8-117-29	LCE1B	Late Cornified Envelope 1B	8

Sample	p53 array_1					p53 array_2					p53 array_3				
	0h	6h	12h	24h	48h	0h	6h	12h	24h	48h	0h	6h	12h	24h	48h
Cy5											7812	0	2944	35114	1E+05
Cy3											10268	45	4927	1195	19871
Cutoff_Cy5											4141	4726	5641	7439	5479
Cutoff_Cy3											4332	4163	5269	694.7	7028
Cy5/Cy3											0.741			29.36	5.853

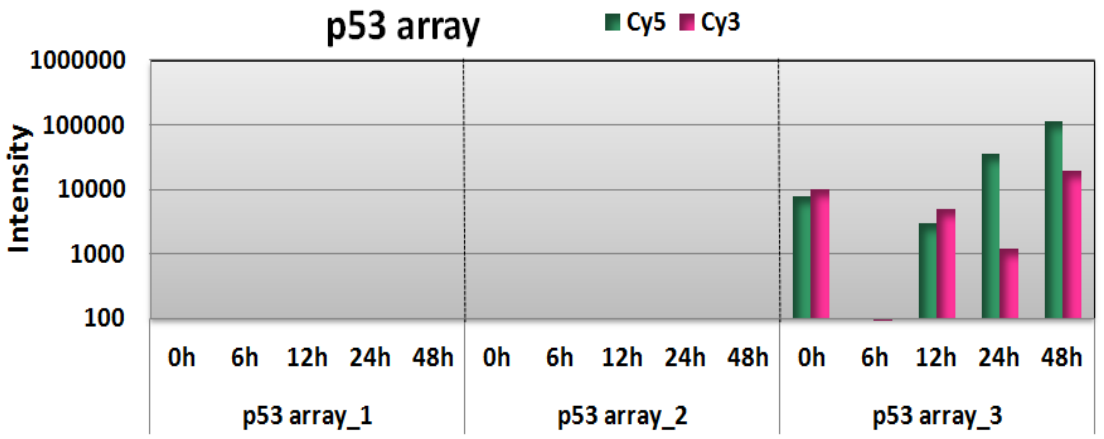

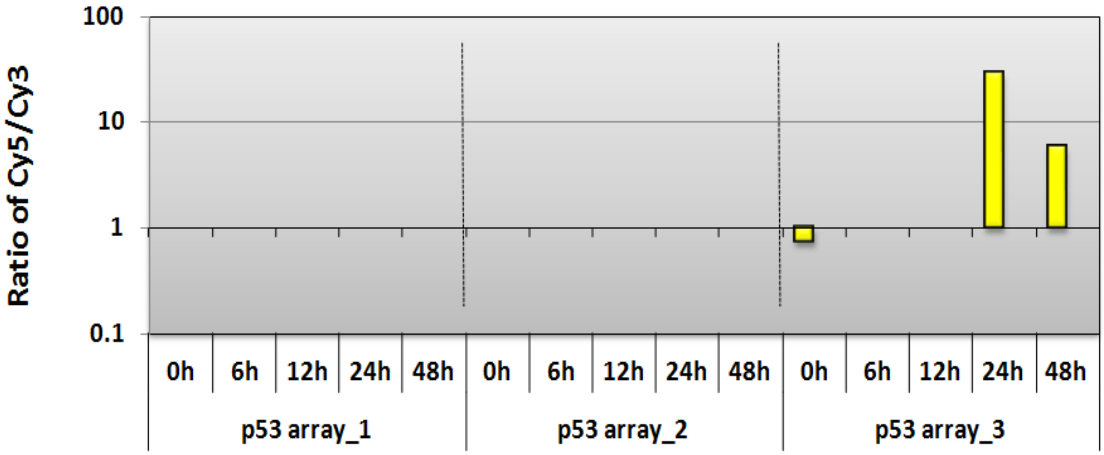

Spot	LMMID	Symbol	Gen Name	Set
H1945	8-143-22	LCE1C	Late Cornified Envelope 1C	8

Sample	p53 array_1					p53 array_2					p53 array_3				
	0h	6h	12h	24h	48h	0h	6h	12h	24h	48h	0h	6h	12h	24h	48h
Cy5											6190	3349	9392	38735	64607
Cy3											8610	4031	8863	4887	14356
Cutoff_Cy5											4141	4726	5641	7439	5479
Cutoff_Cy3											4332	4163	5269	694.7	7028
Cy5/Cy3											0.719		1.06	7.925	4.5

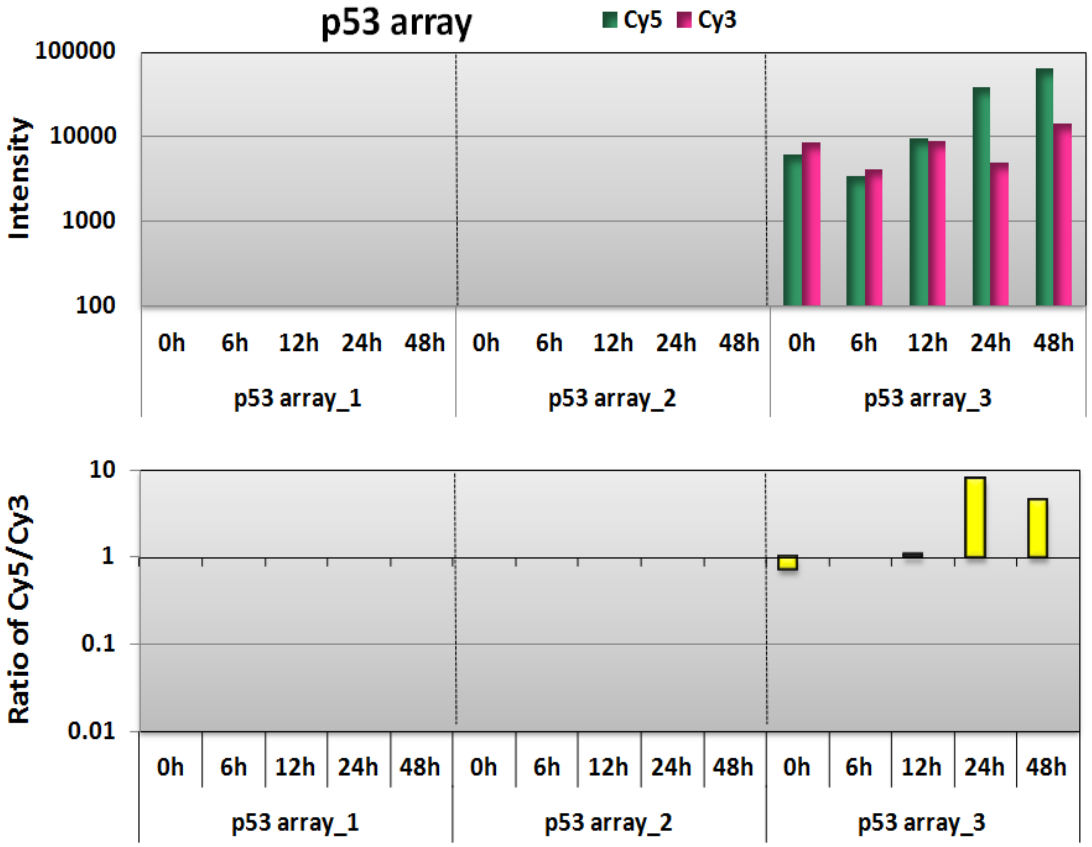

Figure 5. Identification of *LCE1B* and *LCE1C* as p53 downstream genes. Genome-wide cDNA microarray analysis was performed using U373MG (mutant p53) cells after infection with Ad-p53 or Ad-LacZ at 20 MOIs. Expression profiles were analyzed using RNA extracted at 0h, 6h, 12h, 24h and 48h. The ratio of Cy5/Cy3 was calculated by the fluorescence signal intensity of Ad-p53 (labeled by Cy5 in green) and the Ad-LacZ (labeled by Cy3 in red). *LCE1B* and *LCE1C* mRNA were found to be up-regulated more than seven folds by the induction of p53.

LCE1B and *LCE1C* belong to the *LCE* gene cluster containing multiple well-conserved genes that encode stratum-corneum proteins. Within the *LCE* cluster, multiple genes form "groups" at chromosome 1q21 and are known to respond "group-wise" to various environmental stimuli like calcium and ultraviolet (UV) light [9], suggesting that other *LCE* members that were not included in our microarray might also be regulated by p53. I first compared the sequence similarity of the *LCE1B* and *LCE1C* transcripts with other members in the *LCE* cluster (Table 5), and selected genes showing high similarity (>80%) for further validation by quantitative real-time PCR because the microarray results might be reflected the cross-hybridization of other LCE members that were possibly induced by p53. However, since I failed to amplify *LCE1D* by PCR with various sets of primers, *LCE1D* was excluded for further analysis.

Table 5. mRNA similarity of LCE family.

Similarity of mRNA*		1	2
		LCE1B	LCE1C
1	LCE1A	**81**	**81**
2	LCE1B		**82**
3	LCE1C	**82**	
4	LCE1D	**91**	**93**
5	LCE1E	54	**85**
6	LCE1F	**80**	**80**
7	LCE2A	73	71
8	LCE2B	74	69
9	LCE2C	74	72
10	LCE2D	73	70
11	LCE3A	**84**	**84**
12	LCE3B	**84**	77
13	LCE3C	**80**	74
14	LCE3D	70	64
15	LCE3E	65	65
16	LCE4A	**85**	**81**
17	LCE5A	65	66
18	LCE6A	68	51
19	SMCP	61	54
20	CRNN	52	65
21	CRCT1	61	58
22	C1orf45	67	**82**
23	XP33	**85**	69

*Similarity of mRNA sequneces between each LCE member and LCE1B or LCE1C (%) was drawn by clustalw2. Genes in shadowed boxes show the similarity of mRNA over 80%.

Interestingly, expression levels of *LCE1* group genes including *LCE1B, LCE1C, LCE1E* and *LCE1F*, were significantly increased in both U373MG (Figure 6*A*) and H1299 (Figure 6*B*) cells after introduction with wild-type p53 (Table 6) although the induction levels are different among the genes. On the other hand, other genes in the LCE cluster such as *C1orf45, LCE4A, XP33, LCE3A, LCE3B* and *LCE3C* were not induced by the introduction with wild-type p53. In addition, treatment with Adriamycin or UV irradiation, which induces endogenous p53, enhanced expression levels of the *LCE1* group genes, *LCE1A, LCE1B, LCE1C, LCE1E* and *LCE1F*, in HCT116 $p53^{+/+}$ cells, but not in HCT116 $p53^{-/-}$ cells (Table 6, Figures 6*C and* 4*D*), indicating that the LCE1 group genes can respond group-wise to the genotoxic stress condition in a p53-dependent manner [9].

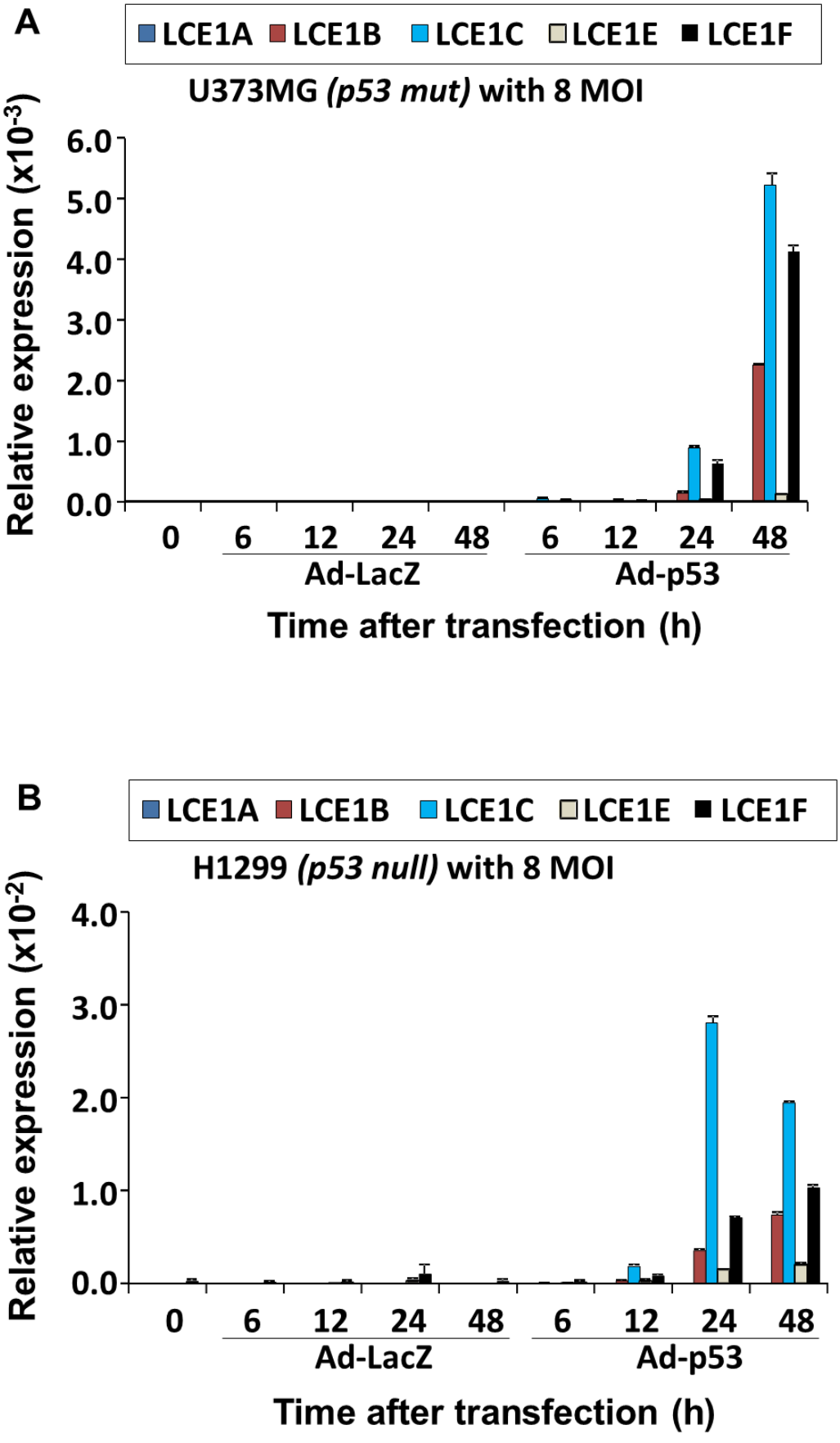
A
LCE1A
LCE1B
LCE1C
LCE1E
LCE1F
U373MG (p53 mut) with 8 MOI
Relative expression (x10-3)
6.0
5.0
4.0
3.0
2.0
1.0
0.0
0
6
12
24
48
6
12
24
48
Ad-LacZ
Ad-p53
Time after transfection (h)
B
LCE1A
LCE1B
LCE1C
LCE1E
LCE1F
H1299 (p53 null) with 8 MOI
Relative expression (x10-2)
4.0
3.0
2.0
1.0
0.0
0
6
12
24
48
6
12
24
48
Ad-LacZ
Ad-p53
Time after transfection (h)

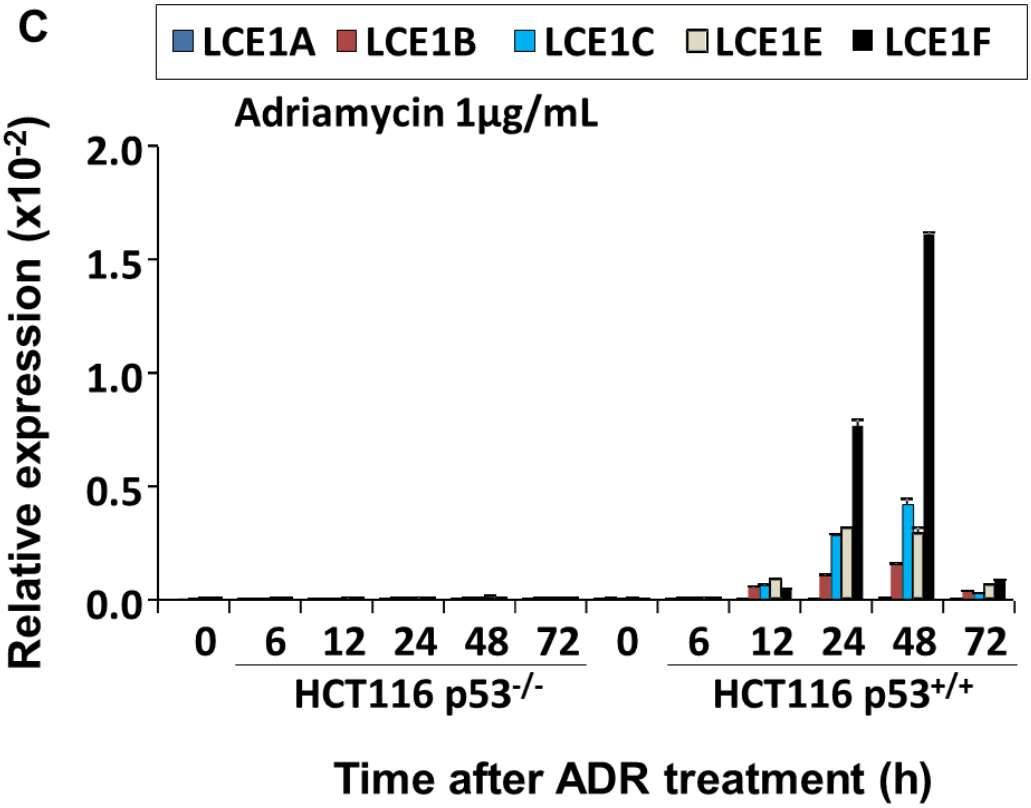
C
LCE1A LCE1B LCE1C LCE1E LCE1F
Adriamycin 1μg/mL
Relative expression (x10-2)
2.0
1.5
1.0
0.5
0.0
0 6 12 24 48 72 0 6 12 24 48 72
HCT116 p53-/-
HCT116 p53+/+
Time after ADR treatment (h)

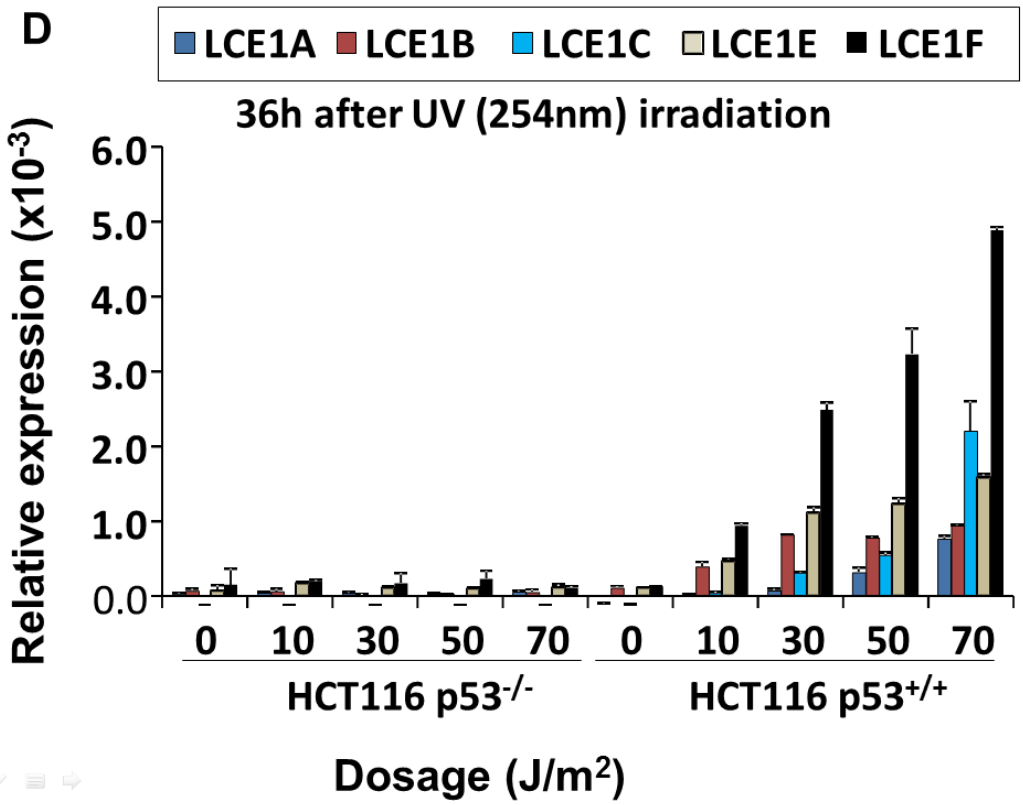
D
LCE1A LCE1B LCE1C LCE1E LCE1F
36h after UV (254nm) irradiation
Relative expression (x10-3)
6.0
5.0
4.0
3.0
2.0
1.0
0.0
0 10 30 50 70 0 10 30 50 70
HCT116 p53-/-
HCT116 p53+/+
Dosage (J/m2)

Figure 6. Expression of *LCE1* genes in response to *p53*, Adriamycin, and UV irradiation. Quantitative real-time PCR analysis of *LCE1* family members was performed in U373MG *(p53 mutant)* (A) and H1299 *(p53 null)* (B) cells at the indicated time points. (C) Time-dependent expression of *LCE1* genes after the treatment with Adriamycin (ADR, 1 μg/ml) in $p53^{-/-}$ and $p53^{+/+}$ HCT116 cells. (D) Dose-dependent expression of *LCE1* genes after the treatment with ultra-violet irradiation (UVR) in $p53^{-/-}$ and $p53^{+/+}$ HCT116 cells. β2-Microglobulin was used for the normalization of expression levels.

Table 6. Expression of *LCE* cluster genes in response to *p53*, Adriamycin, and UVR

(A) Response to Ad-LacZ or Ad-p53 in U373MG cells

Expression	Time points	U373MG by Ad-LacZ			
Genes	0h	6h	12h	24h	48h
LCE1A	4.39E-07	3.57E-07	1.80E-07	1.43E-07	1.00E-07
LCE1B	1.64E-07	2.05E-07	1.54E-07	4.44E-07	1.79E-08
LCE1C	2.42E-07	2.90E-07	ND	5.95E-07	1.13E-06
LCE1E	2.04E-07	3.30E-07	3.35E-07	3.64E-07	3.08E-07
LCE1F	7.06E-08	1.61E-07	ND	6.56E-08	3.88E-07
LCE3A	4.29E-06	4.78E-06	3.37E-06	3.77E-06	3.13E-06
LCE3B	2.91E-06	2.33E-06	1.49E-06	ND	ND
LCE3C	ND	ND	ND	ND	ND
LCE4A	ND	ND	ND	2.21E-09	1.05E-09
C11orf45	2.04E-06	4.14E-06	ND	ND	ND
XP33	3.11E-09	ND	1.90E-09	1.12E-09	ND

Expression	Time points	U373MG by Ad-p53			
Genes	0h	6h	12h	24h	48h
LCE1A	4.39E-07	2.02E-07	2.08E-07	1.77E-07	3.02E-07
LCE1B	1.64E-07	1.39E-06	3.50E-06	1.55E-04	2.26E-03
LCE1C	2.42E-07	5.79E-05	2.78E-05	9.00E-04	5.24E-03
LCE1E	2.04E-07	1.98E-06	2.31E-06	3.24E-05	1.28E-04
LCE1F	7.06E-08	3.70E-05	1.39E-05	6.29E-04	4.13E-03
LCE3A	4.29E-06	3.90E-06	3.83E-06	4.05E-06	2.83E-06
LCE3B	2.91E-06	4.46E-06	4.77E-06	5.93E-06	9.50E-06
LCE3C	ND	ND	ND	ND	ND
LCE4A	ND	1.81E-08	2.64E-09	1.37E-08	7.11E-09
C11orf45	2.04E-06	ND	ND	ND	1.20E-06
XP33	3.11E-09	3.36E-09	3.98E-09	3.12E-09	ND

(B) Response to Ad-LacZ or Ad-p53 in H1299 cells

Expression	Time points	H1299 by Ad-LacZ			
Genes	0h	6h	12h	24h	48h
LCE1A	ND	ND	ND	ND	ND
LCE1B	ND	ND	ND	ND	ND
LCE1C	ND	ND	ND	ND	ND
LCE1E	ND	ND	ND	1.29E-04	ND
LCE1F	2.79E-04	2.02E-04	2.28E-04	1.05E-03	2.61E-04

Expression	Time points	H1299 by Ad-p53			
Genes	0h	6h	12h	24h	48h
LCE1A	ND	ND	ND	ND	ND
LCE1B	ND	1.13E-05	3.20E-04	3.55E-03	7.37E-03
LCE1C	ND	ND	1.84E-03	2.81E-02	1.95E-02
LCE1E	ND	4.21E-06	3.22E-04	5.24E-04	7.73E-04
LCE1F	2.79E-04	2.26E-04	8.14E-04	7.10E-03	1.03E-02

(C) Response to ADR in HCT116 $p53^{-/-}$ and HCT116 $p53^{+/+}$ cells.

Expression	HCT116 $p53^{-/-}$ by ADR at 1μg/mL					
Genes	0h	6h	12h	24h	48h	72h
LCE1A	9.51E-07	2.31E-07	4.39E-07	7.41E-07	2.49E-06	2.01E-06
LCE1B	6.12E-06	3.59E-06	3.32E-06	7.12E-06	2.24E-05	9.77E-06
LCE1C	8.33E-07	8.11E-07	3.84E-06	7.22E-06	2.13E-05	1.85E-05
LCE1E	1.09E-05	5.11E-06	2.81E-05	1.79E-05	1.20E-04	2.76E-05
LCE1F	1.70E-05	7.19E-06	7.56E-06	5.17E-06	1.86E-05	1.39E-05

Expression	HCT116 $p53^{+/+}$ by ADR at 1μg/mL					
Genes	0h	6h	12h	24h	48h	72h
LCE1A	1.49E-07	1.41E-07	1.04E-06	1.90E-06	6.19E-06	1.27E-06
LCE1B	6.85E-06	3.05E-05	7.69E-04	1.42E-03	2.10E-03	4.04E-04
LCE1C	1.51E-06	7.65E-06	6.09E-04	2.82E-03	4.16E-03	2.41E-04
LCE1E	1.09E-05	3.78E-05	8.68E-04	3.13E-03	2.88E-03	6.14E-04
LCE1F	2.90E-06	9.23E-06	4.46E-04	7.62E-03	1.60E-02	8.02E-04

(D) Response to UVR in HCT116 $p53^{-/-}$ and HCT116 $p53^{+/+}$ cells.

Expression	HCT116 $p53^{-/-}$ UVR				
Genes	0 J/m^2	10 J/m^2	30 J/m^2	50 J/m^2	70 J/m^2
LCE1A	1.30E-05	2.63E-06	3.37E-06	2.46E-06	3.42E-06
LCE1B	ND	1.49E-06	ND	9.56E-07	ND
LCE1C	4.89E-06	ND	3.23E-06	4.65E-06	1.77E-06
LCE1E	1.82E-05	1.68E-05	7.52E-06	7.96E-06	3.70E-06
LCE1F	7.38E-05	4.14E-05	2.78E-05	3.56E-05	3.16E-05
LCE3A	2.75E-04	1.84E-04	9.97E-05	1.10E-04	9.00E-05
LCE3B	2.76E-04	1.62E-04	1.07E-04	1.18E-04	1.42E-04
LCE3C	ND	ND	ND	ND	ND
LCE4A	4.58E-04	3.83E-04	1.67E-04	1.86E-04	1.57E-04
C11orf45	ND	ND	ND	ND	ND
XP33	5.25E-06	2.29E-05	7.19E-06	3.63E-06	9.62E-06

Expression	HCT116 $p53^{+/+}$ UVR				
Genes	0 J/m^2	10 J/m^2	30 J/m^2	50 J/m^2	70 J/m^2
LCE1A	2.44E-06	1.58E-06	7.60E-05	1.13E-04	9.60E-05
LCE1B	2.91E-05	1.40E-04	1.75E-04	2.13E-04	2.72E-04
LCE1C	5.18E-06	5.13E-05	1.34E-04	2.21E-04	3.62E-04
LCE1E	1.47E-05	1.19E-04	1.81E-04	2.86E-04	4.86E-04
LCE1F	2.92E-05	1.39E-04	3.07E-04	4.09E-04	6.14E-04
LCE3A	2.72E-05	3.28E-05	2.37E-05	3.30E-05	2.10E-05
LCE3B	3.85E-05	4.68E-05	2.71E-05	2.89E-05	4.28E-05
LCE3C	ND	ND	ND	ND	ND
LCE4A	6.56E-05	1.33E-04	5.82E-05	6.31E-05	6.41E-05
C11orf45	ND	ND	ND	ND	ND
XP33	6.15E-07	8.81E-07	5.37E-07	5.60E-07	4.17E-07

Quantitative real-time PCR analysis of *LCE* cluster genes in U373MG *(p53 mutant)* (A) and H1299 *(p53 null)* (B) cells at indicated time points after infection with Ad-p53 or Ad-LacZ at 8 MOIs. (C) Expression of *LCE1* genes in $p53^{-/-}$ and $p53^{+/+}$ HCT116 cells after treatment with Adriamycin (ADR, 1 μg/ml) at indicated time points.
(D) Expression of *LCE1* genes in $p53^{-/-}$ and $p53^{+/+}$ HCT116 cells after treatment with UVR at different doses. β2-Microglobulin was used for the normalization of expression levels. ND, not detectable levels.

LCE1F Is a Direct Target of p53

I then attempted to clarify whether *LCE1* genes are directly or indirectly regulated by p53. First, I searched for putative p53-binding sites (p53BSs) in the genomic region of the *LCE1* cluster, and identified a total of eleven p53BSs containing at least 80% of 20 nucleotides in the two halves of consensus p53 binding sequence (*see* Materials and Methods) (Table 7 and Figure 7A) and confirmed at least one site that was likely to be a direct p53-binding sequence (Figure 7).

Reporter plasmids containing one or two of the 11 p53BSs were prepared (Figure 7*A*) and a reporter assay was performed with the reporter plasmids with or without wild type p53 plasmids in U373MG cells and H1299 cells. Consequently, luciferase activity of p53BS2, p53BS6, and p53BS7 was enhanced by co-transfection with wild-type p53 in both U373MG (Figure 7*B*) and H1299 cells (Figure 7*C*). I further investigated the specificity of these three p53BSs by the nucleotide substitutions of the core consensus sequence (Figure 8*A*). As a result, I observed that substitutions in either of the p53BS2, p53BS6 and p53BS7 sequences significantly diminished the enhancement of the luciferase activity in both U373MG and H1299 cells (Figures 8*B* and 8*C*).These results suggested that these p53-binding regions are essential for the induction of *LCE1* cluster genes.

Table 7. Predicted p53-binding sequences within the *LCE1* cluster region

	Sequence*	Physical Position Dec. 2013 (GRCh38/hg38)
p53BS1	A G c C T A G g C T A A t C T T G T T C	Chr1: 152768000-152768019
p53BS2	A G G C A g G T C C t c t C A T G C C C	Chr1: 152775052-152775071
p53BS3	G C a C A A G C T g G t G C T g G C C C	Chr1: 152777516-152777535
p53BS4	G G G C A A G T C C t c t C A T G C C C	Chr1: 152786169-152786188
p53BS5	A t G C A T G T g T G t G C A T G T T T	Chr1: 152804402-152804421
p53BS6	G G G C A T G a g a G G A C c T G C C T	Chr1: 152806719-152806738
p53BS7	A G G C A A G T C C t c t C A T G C C C	Chr1: 152811261-152811280
p53BS8	T A A C T T G g T g A G A C A A GT a C	Chr1: 152811810-152811829
p53BS9	c t G C A g G T T T A A A C T g G C T C	Chr1: 152827076-152827095
p53BS10	A c A C T T G C T C A G G g A A G G TG	Chr1: 152789730-152789749
p53BS11	A G A C A A G C C T G A G C A A c a T a	Chr1: 152791868-152791887

*Identical nucleotides to the p53-binding motif are written in capital letters.

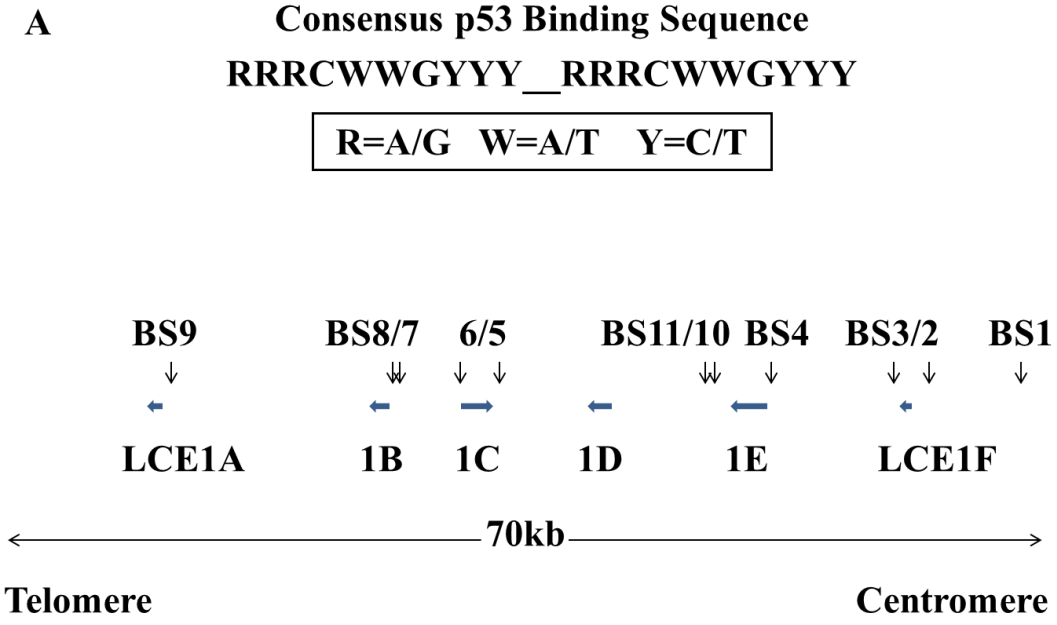
A
Consensus p53 Binding Sequence
RRRCWWGYYY__RRRCWWGYYY
R=A/G W=A/T Y=C/T
BS9
BS8/7
6/5
BS11/10
BS4
BS3/2
BS1
LCE1A
1B
1C
1D
1E
LCE1F
70kb
Telomere
Centromere

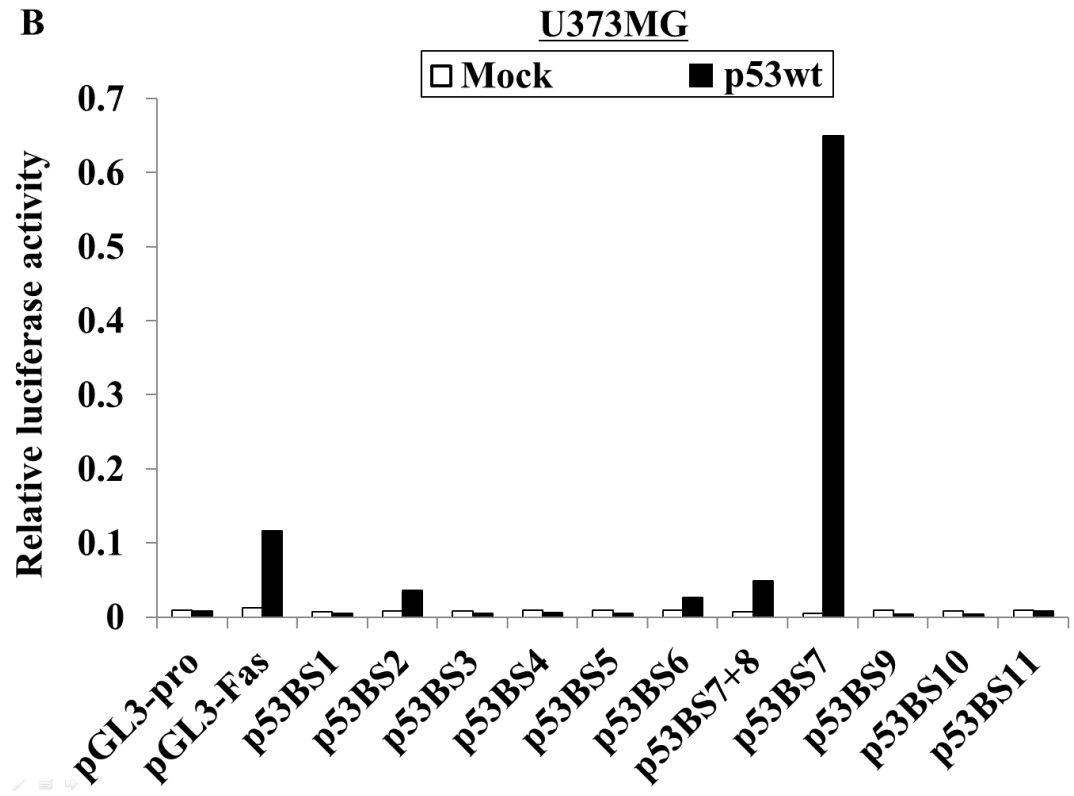
B
U373MG
Mock
p53wt
Relative luciferase activity
0.7
0.6
0.5
0.4
0.3
0.2
0.1
0
pGL3-pro
pGL3-Fas
p53BS1
p53BS2
p53BS3
p53BS4
p53BS5
p53BS6
p53BS7+8
p53BS7
p53BS9
p53BS10
p53BS11

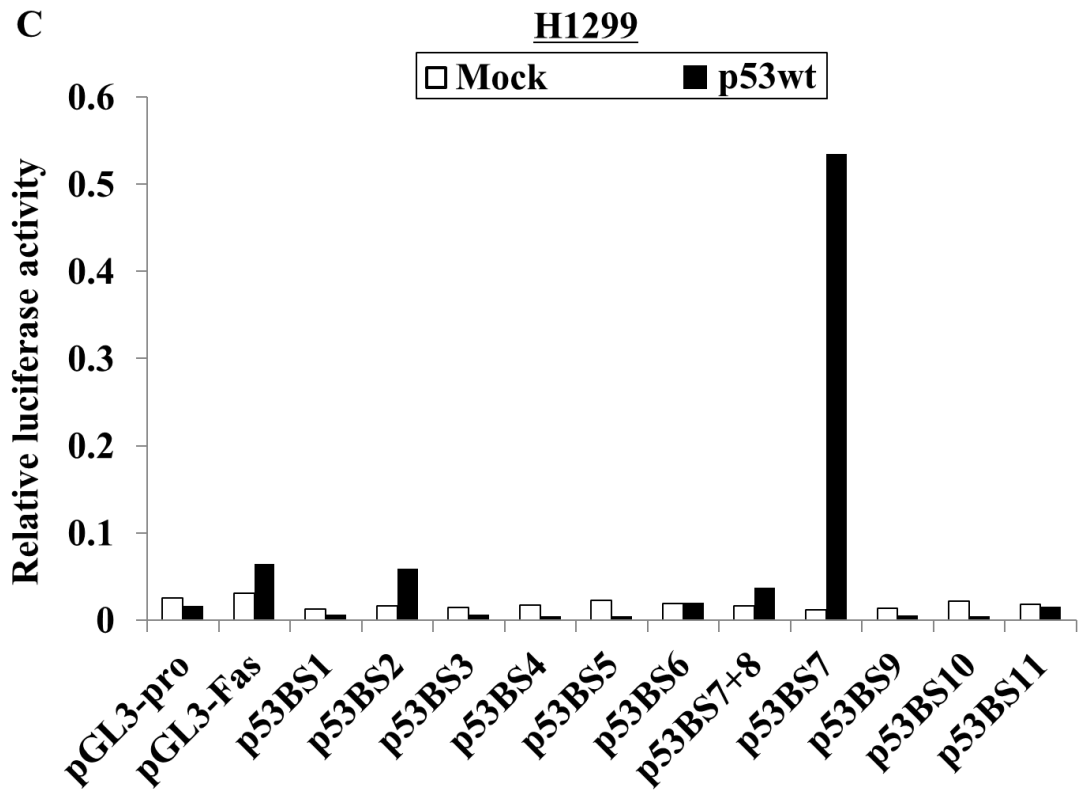

Figure 7. Localization and characterization of the predicted p53-binding sequences. (A) Eleven potential p53 binding sequences (p53BS) were predicted in the *LCE1* gene cluster region. Bold horizon arrows indicate the locations and relative sizes of each *LCE1* gene. Vertical arrows show the locations of the eleven p53BS. (B, C) Reporter assays with the reporter plasmids containing one or two of p53BS in the presence (p53wt) or absence (Mock) of wild-type p53 in U373MG (B) and H1299 (C) cells.

A

Consensus p53 Binding Sequence

RRRCWWGYYY__RRRCWWGYYY

R=A/G W=A/T Y=C/T

	Sequence	match
p53BS2	AGGCAgGTCCtctCATGCCC	16/20
p53BS2 mut	AGGTAgTTCCtctTATTCCC	12/20
p53BS6	GGGCATGagaGGACcTGCCT	16/20
p53BS6 mut	GGGTATTagaGGATcTTCCT	12/20
p53BS6-	TCCGTcCAGGagaGTACGGG	16/20
p53BS6-mut	TCCTTcTAGGagaTTATGGG	12/20
p53BS7	AGGCAAGTCCtctCATGCCC	17/20
p53BS7 mut	AGGTAATTCCtctTATTCCC	13/20
p53BS7-	CCCGTACtctCCTGAACGGA	17/20
p53BS7-mut	CCCTTATtctCCTTAATGGA	13/20

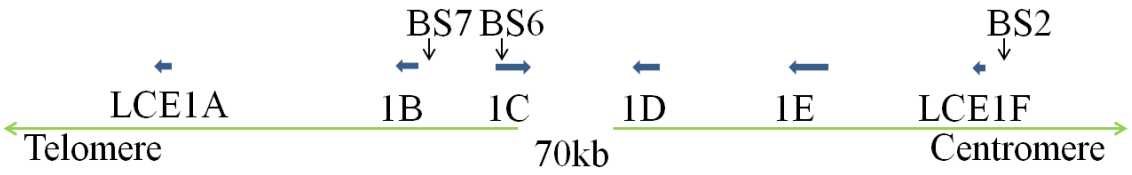

B

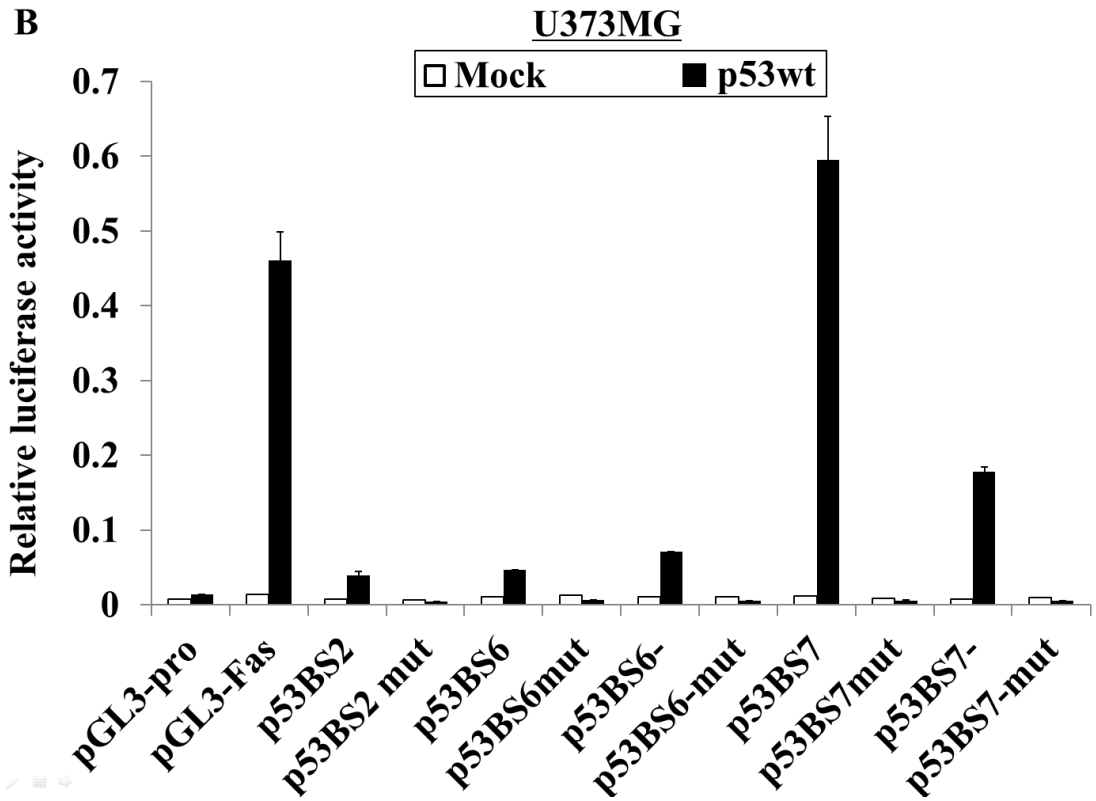

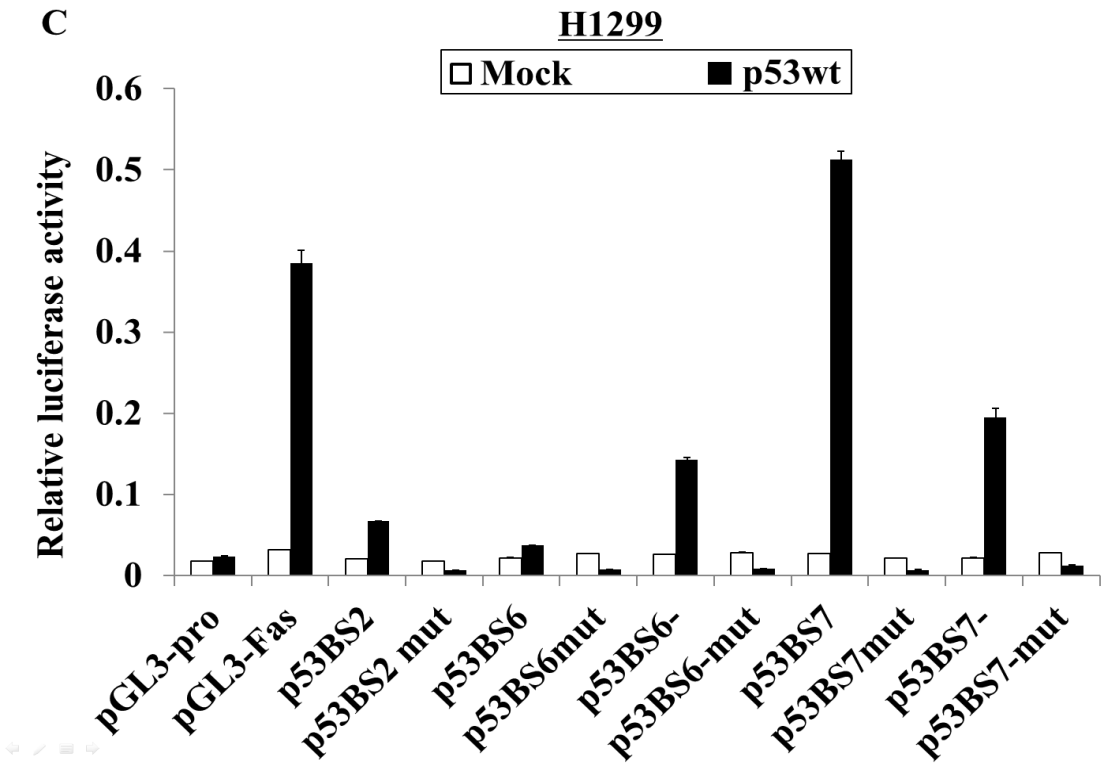
C
H1299
Mock
p53wt
Relative luciferase activity
0.6
0.5
0.4
0.3
0.2
0.1
0
pGL3-pro
pGL3-Fas
p53BS2
p53BS2 mut
p53BS6
p53BS6mut
p53BS6-
p53BS6-mut
p53BS7
p53BS7mut
p53BS7-
p53BS7-mut

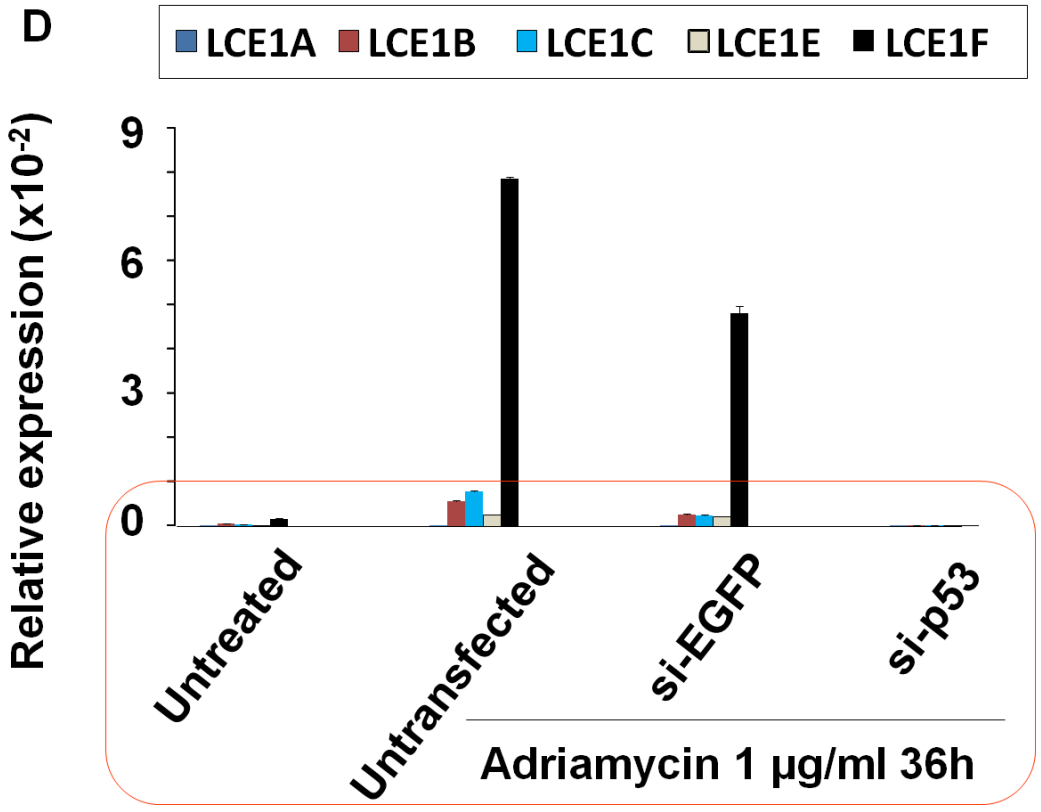
D
LCE1A
LCE1B
LCE1C
LCE1E
LCE1F
Relative expression (x10-2)
9
6
3
0
Untreated
Untransfected
si-EGFP
si-p53
Adriamycin 1 μg/ml 36h

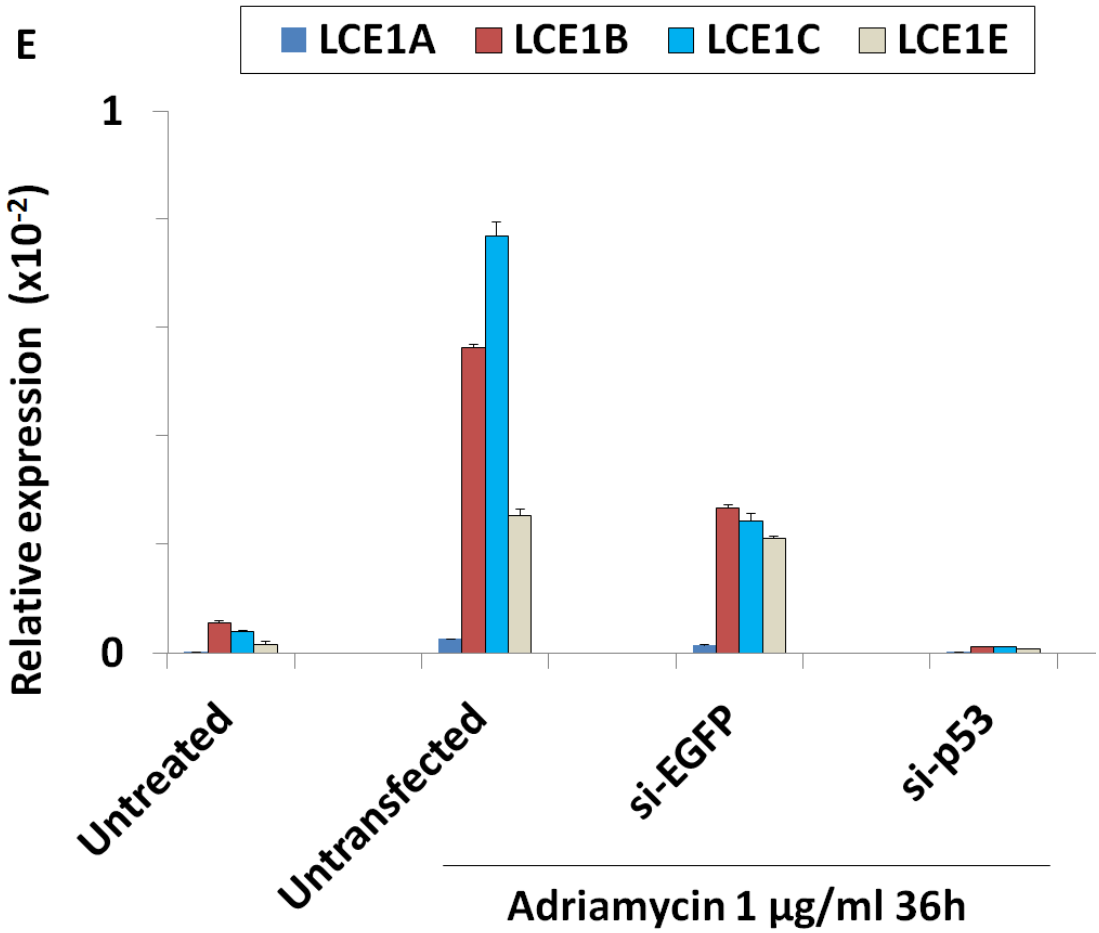

Figure 8. Specific induction of the reporter activity containing the predicted p53BS. (A) Reporter plasmids containing mutant p53-binding sites (p53BS2, p53B6, p53B6-, p53BS7, and p53BS7-) I focused on three p53-binding sites because these regions are associated with induction of *LCE1* genes as shown in Figure 7. The underlined nucleotides indicate the substitution of cytosine or guanine. (B, C) Reporter assays of wild-type and mutant p53-binding sites in U373MG (B) and H1299 (C) cells. Results are shown as the firefly luciferase activity normalized by the Renilla luciferase activity. (D, E) Real-time qPCR of *LCE1* family genes. HCT116 $p53^{+/+}$ cells were transfected with siRNAs targeting EGFP or p53 for 24 h and treated with ADR. (E) The detailed expression of *LCE1A*, *LCE1B*, *LCE1C* and *LCE1E* gated by square in (D).

To confirm the p53-dependent induction of LCE1 genes, I treated the HCT116 $p53^{+/+}$ cells with p53-specific siRNA or control siRNA (siEGFP) after the incubation with Adriamycin. Consistent with Figure 6C, genotoxic stress by Adriamycin remarkably enhanced the expression of *LCE1A*, *LCE1B*, *LCE1C*, *LCE1E*, and *LCE1F*, and siRNA to p53 significantly suppressed their induction (Figures 8*D* and 8*E*). These data implied that expression levels of *LCE1A*, *LCE1B*, *LCE1C*, *LCE1E*, and *LCE1F* are regulated by a p53-dependent manner.

To investigate a possible association of the three p53BSs with p53, I additionally performed chromatin immunoprecipitation (ChIP) analysis, and found that p53 associated with p53-BS2 in the *LCE1* cluster region in HCT116 $p53^{+/+}$ cells treated with Adriamycin (Figure 9).

I additionally examined the expression levels of *LCE1F* in 60 cancer cell lines by quantitative real-time PCR (Table 8), and revealed that *LCE1F* expression was relatively lower in p53 mutant (mut) cells compared with p53 wild-type (wt) cells among the colon and lung cancer cell lines I examined (Figure 10). This is consistent with the notion that *LCE1F* is a direct p53-target gene as shown in Figure 7.

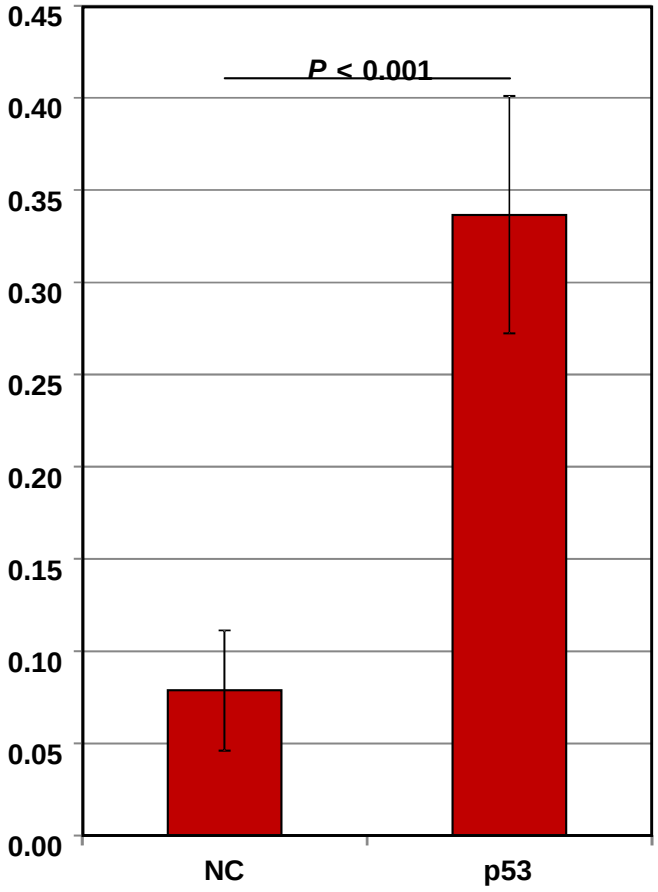

Figure 9. Chromatin immunoprecipitation (ChIP) assay for the p53BS2 region

Real-time qPCR assay of immunoprecipitants with anti-p53 antibody was performed. Precipitants with protein A agarose/Salmon Sperm DNA were used for the negative control (NC). Results are shown as a percentage of the PCR products with the input. Data are presented with the mean ±SD of three independent experiments. The *P* value was calculated using Student's *t*-test.

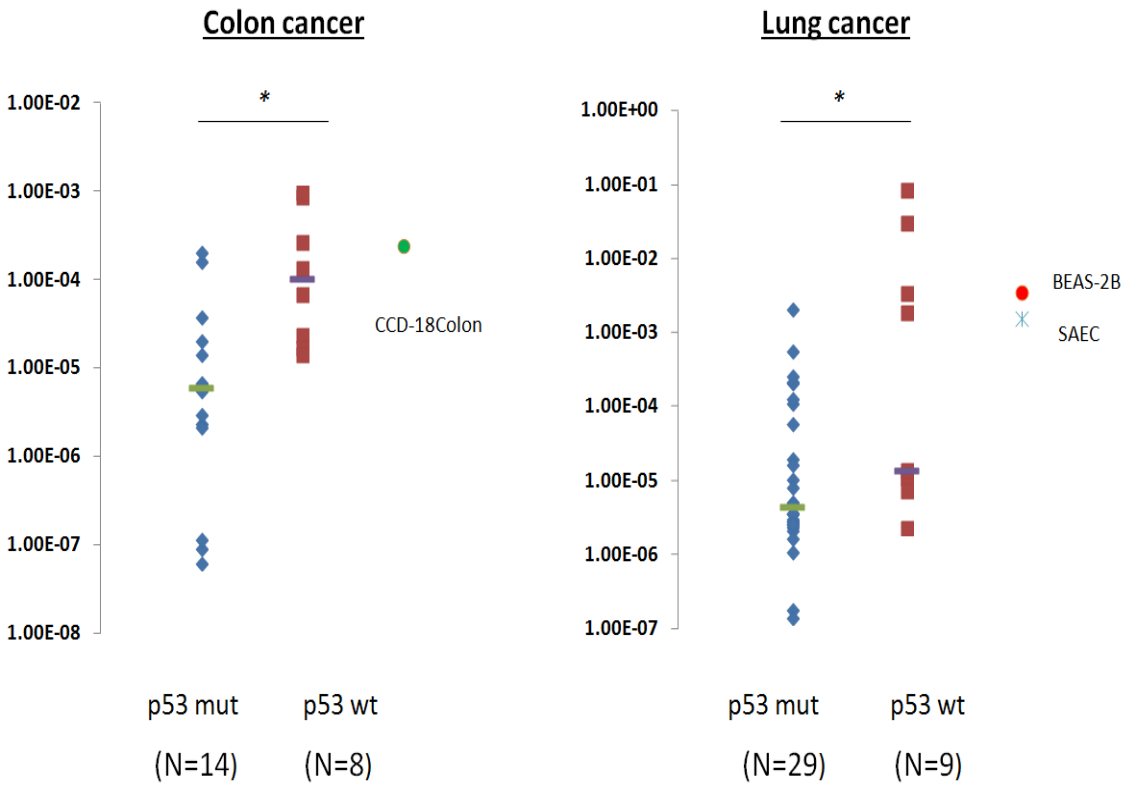

Figure 10. Expression levels of *LCE1F* in 60 cancer cell lines.

Real-time qPCR analysis was performed to examine the expression levels of *LCE1F* in 60 cancer cell lines listed in Table 8. The vertical means the median value of expression levels of *LCE1F* in each group. β2-Microglobulin (*B2M*) was used for the normalization of expression levels. Asterisks indicate significant difference of *P*-value calculated by Student's *t*-test: $*P < 0.05$.

Table 8. Expression of LCE1F in 60 cancer cell lines.

	Cell line	p53 status	LCE1F expression	Origin
1	DLD-1	mut	2.33E-06	Colon
2	HCT-15	mut	5.49E-06	Colon
3	HT-29	mut	6.58E-06	Colon
4	KM12C	mut	2.89E-06	Colon
5	KM12SM	mut	1.39E-05	Colon
6	NCI-H508	mut	6.67E-06	Colon
7	NCI-H684	mut	8.85E-08	Colon
8	NCI-H716	mut	1.14E-07	Colon
9	SNU-C2A	mut	6.12E-08	Colon
10	SNU C5	mut	1.98E-05	Colon
11	SW480	mut	1.57E-04	Colon
12	SW620	mut	1.98E-04	Colon
13	SW948	mut	3.73E-05	Colon
14	WiDr	mut	2.10E-06	Colon
15	HCT 116	wt	1.34E-04	Colon
16	LoVo	wt	2.35E-05	Colon
17	LS 174T	wt	6.80E-05	Colon
18	NCI-H498	wt	8.66E-04	Colon
19	NCI-H747	wt	2.68E-04	Colon
20	RKO	wt	9.60E-04	Colon
21	SNU C4	wt	1.72E-05	Colon
22	SW48	wt	1.42E-05	Colon
23	CCD-18Co	wt	2.41E-04	Normal Epithelium of Colon

	Cell line	p53 status	LCE1F expression	Origin
1	DMS 114	mut	1.10E-04	Lung
2	DMS 273	mut	3.60E-06	Lung
3	LC174	mut	2.07E-04	Lung
4	NCI-H358	mut	2.34E-06	Lung
5	NCI-H522	mut	2.18E-04	Lung
6	NCI-H596	mut	4.46E-06	Lung
7	Pc-3	mut	1.81E-07	Lung

8	SK-LU-1	mut	2.79E-06	Lung
9	SK-MES-1	mut	3.04E-06	Lung
10	PC14	mut	5.13E-06	Lung
11	PERF-LC-AI	mut	2.13E-06	Lung
12	NCI-H1703	mut	1.40E-07	Lung
13	EBC-1	mut	3.57E-06	Lung
14	LU61	mut	2.02E-03	Lung
15	SBC-5	mut	2.56E-04	Lung
16	NCI-H1299	mut	5.85E-05	Lung
17	NCI-H446	mut	2.77E-06	Lung
18	NCI-H196	mut	2.53E-06	Lung
19	NCI-H1373	mut	1.09E-06	Lung
20	NCI-H1650	mut	1.04E-05	Lung
21	NCI-H1781	mut	1.93E-05	Lung
22	NCI-H2170	mut	4.85E-06	Lung
23	NCI-H23	mut	5.67E-04	Lung
24	NCI-H520	mut	8.06E-06	Lung
25	NCI-H647	mut	3.58E-06	Lung
26	LX1	mut	1.28E-04	Lung
27	PC14PE6	mut	1.61E-05	Lung
28	RERF-LC-AI	mut	1.66E-06	Lung
29	SW900	mut	2.65E-06	Lung
30	A549	wt	2.28E-06	Lung
31	LC176	wt	1.10E-05	Lung
32	LU99A	wt	1.11E-05	Lung
33	LU99B	wt	1.38E-05	Lung
34	NCI-H226	wt	1.83E-03	Lung
35	NCI-H460	wt	7.36E-06	Lung
36	SBC-3	wt	8.54E-02	Lung
37	A427	wt	2.99E-02	Lung
38	SW1573	wt	3.40E-03	Lung
39	SAEC	Wt	1.52E-03	Normal Epithelium of Lung
40	BEAS-2B	wt	3.52E-03	Normal Epithelium of Lung

Subcellular localization of LCE1F

To clarify the function of LCE1F in cancer cells, I first examined the subcellular localization of LCE1F by immunocytochemical staining. I expressed HA-tagged full-length LCE1F protein in HEK293T cells. Although the predicted molecular weight of HA-tagged LCE1F was 13 kDa, we detected a band corresponding to the protein at 17 kDa by size by western blot analysis (Figure 11*A*). As shown in Figure 11*B*, immunocytochemical analysis revealed that LCE1F was strongly stained in both nucleus and cytoplasm.

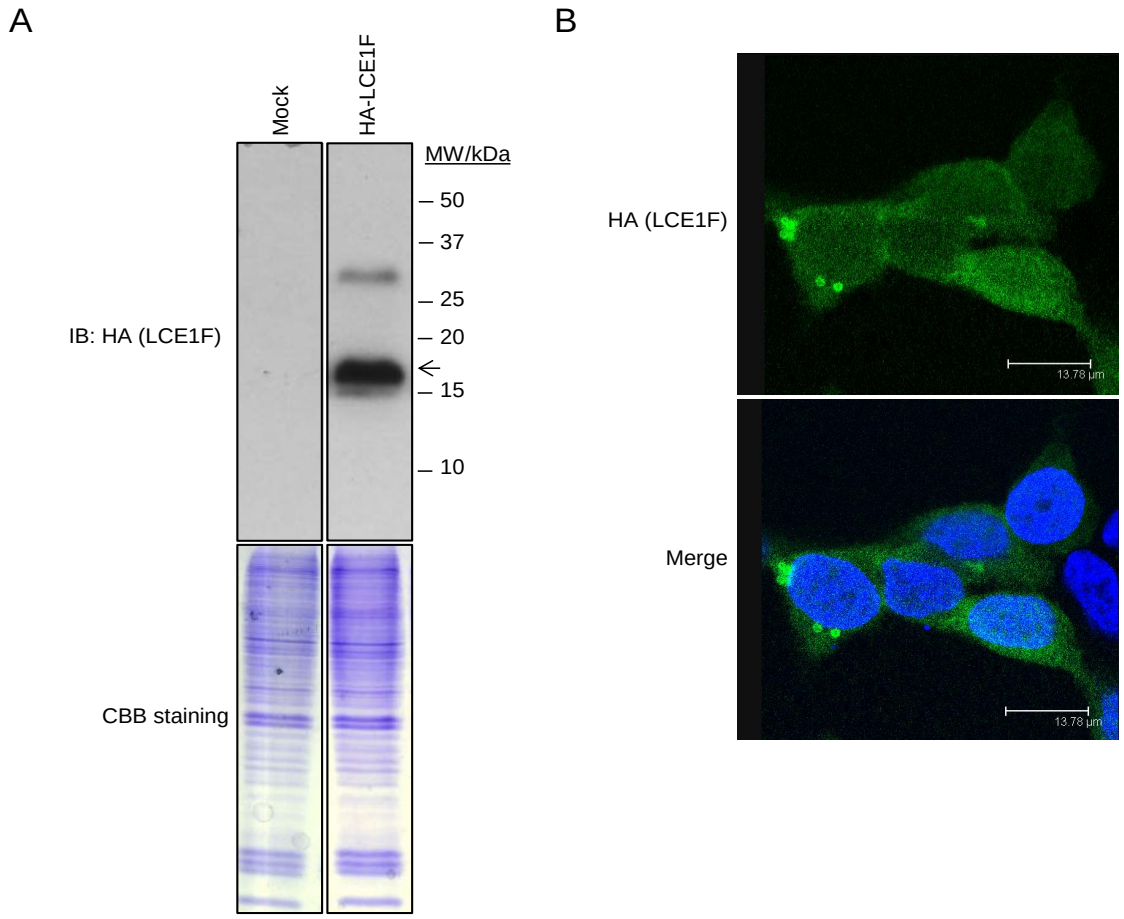

Figure 11. Subcellular localization of HA-tagged LCE1F protein. HEK293T cells were transfected with plasmids expressing HA-tagged LCE1F. (A) Immunoblot analysis of the extracts with an anti-HA antibody. CBB staining was shown as the control of loading protein amount. (B) Immunocytochemical analysis of HA-tagged LCE1F. HA-tagged LCE1F was stained with an anti-HA antibody and visualized with a secondary antibody (green). Nuclei were counter-stained with DAPI (Blue). Scale bars, 13.78 µm.

LCE1F Interacts with PRMT5

Next, I challenged to identify interacting proteins of LCE1 proteins. I transfected HEK293T cells with plasmids expressing HA-tagged LCE1A-F proteins (pCAGGSnHC-LCE1A, LCE1B, LCE1C, LCE1E and LCE1F), and lysates of the cells were immunoprecipitated with anti-HA conjugated agarose beads. Precipitants were separated by SDS-PAGE, and the gel was silver stained (Figure 12). Therefore, I found various bands that were not observed in the precipitants of HA-Mock but observed in those of HA-LCE1A, HA-LCE1B, HA-LCE1C, HA-LCE1E and HA-LCE1F (Figure 12). Among them, I chose four bands, #1(~100 kDa), #2(~70 kDa), #3(~37 kDa) and #4 (~30 kDa) and conducted liquid chromatography-tandem mass spectrometry analysis of these proteins. Since LCE1A, LCE1B, LCE1C, LCE1E and LCE1F showed a high level of amino-acid similarity (Table 10), I did not attempt to identify specific binding proteins. LC-MS analysis identified a set of candidates for each protein with different prediction scores. From the list of candidates, I selected PRMT5, an arginine methyltransferase, because it had a relatively high prot score, and the expected molecular weight matched to the band excised.

Importantly, LCE1 family proteins show a high level of sequence similarity and LCE1F has more than 90% homology with other members (LCE1A-E, Table 10).

Because LCE1F is highly and directly up-regulated by p53 (Figure 6), I chose it for the further functional analysis.

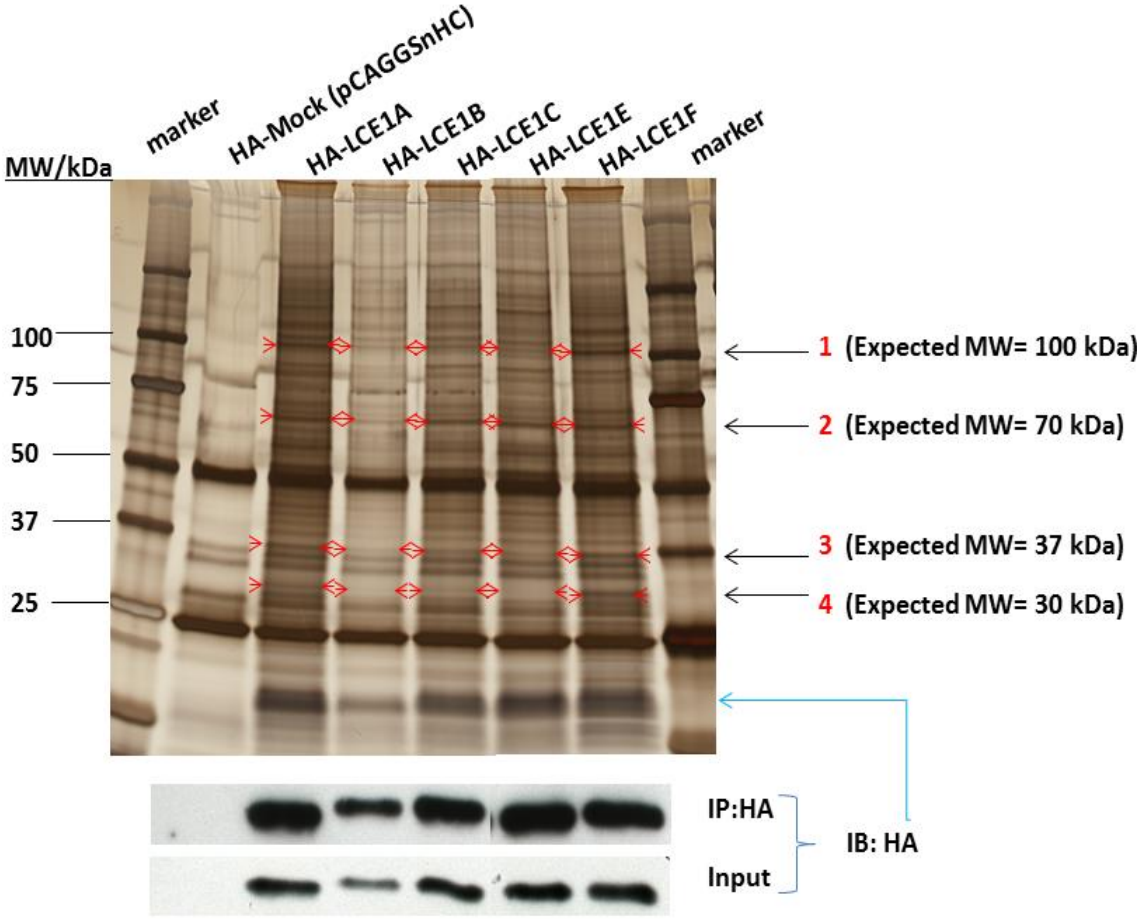

Figure 12. LC-MS analysis for the identification of interacting proteins to HA-tagged LCE1A, LCE1B, LCE1C, LCE1E and LCE1F. Immunoprecipitants from the cells expressing HA-tagged LCE1A, LCE1B, LCE1C, LCE1E and LCE1F were separated by SDS-PAGE and the gel was stained with silver staining kit (upper panel). Four protein samples were extracted from the bands #1, #2, #3, and #4. Western blot analysis of the precipitants with anti-HA antibody (lower panel).

Table 9. List of candidate interacting proteins for the four samples

Sample 1 (Expected MW = 100 kDa)				
prot_ hit_No	***prot_acccession**	**prot_description**	****prot _score**	**prot_ Mass**
1	NUCL_HUMAN	Nucleolin	188	76625
2	CAPR1_HUMAN	Caprin-1	90	78489
3	NCRP1_HUMAN	Non-specific cytotoxic cell receptor protein 1 homolog	52	30942
4	XRN2_HUMAN	5' - 3' exoribonuclease 2	40	1E+05
5	GLRX1_HUMAN	Glutaredoxin-1	34	12053
6	TGM3_HUMAN	Protein-glutamine gamma-glutamyltransferase E	33	76926
7	DDAH2_HUMAN	N^G,N^G -di-methyl arginine di-methyl aminohydrolase 2	26	29911
8	DDX20_HUMAN	Probable ATP-dependent RNA helicase DDX20	25	92981
9	MTAP_HUMAN	S-methyl-5~-thioadenosine phosphorylase	24	31729
10	TERF2_HUMAN	Telomeric repeat-binding factor 2	24	55688
11	S10A9_HUMAN	Protein S100-A9	23	13291
12	NSMA_HUMAN	Sphingomyelin phosphodiesterase 2	19	48128
13	EMAL5_HUMAN	Echinoderm microtubule-associated protein-like 5	19	2E+05
14	ADA30_HUMAN	Disintegrin and metalloproteinase domain-containing protein 30	18	91391
15	SLTM_HUMAN	SAFB-like transcription	18	1E+05

		modulator		
16	C1TC_HUMAN	C-1-tetrahydrofolate synthase, cytoplasmic	17	1E+05
17	F192A_HUMAN	Protein FAM192A	17	29123
18	PPGB_HUMAN	Lysosomal protective protein	17	54944
19	G3P_HUMAN	Glyceraldehyde-3-phosphate dehydrogenase	17	36201
20	CH60_HUMAN	60 kDa heat shock protein, mitochondrial	16	61187
21	DDX10_HUMAN	Probable ATP-dependent RNA helicase DDX10	14	1E+05
Sample 2 (Expected MW = 70 kDa)				
prot_ hit_No	**prot_acccession**	**prot_description**	**prot_sc ore**	**prot_ Mass**
1	HSP71_HUMAN	Heat shock 70 kDa protein 1A/1B	241	70294
2	HSP7C_HUMAN	Heat shock cognate 71 kDa protein	126	71082
3	ANM5_HUMAN	Protein arginine N-methyltransferase 5	117	73322
4	LRC47_HUMAN	Leucine-rich repeat-containing protein 47	100	64004
5	DDX17_HUMAN	Probable ATP-dependent RNA helicase DDX17	75	80906
6	THNS1_HUMAN	Threonine synthase-like 1	62	84100
7	GUAA_HUMAN	GMP synthase [glutamine-hydrolyzing]	56	77408
8	SYRC_HUMAN	Arginine--tRNA ligase, cytoplasmic	52	76129
9	IF2B1_HUMAN	Insulin-like growth factor 2 mRNA-binding protein 1	50	63783
10	FUS_HUMAN	RNA-binding protein FUS	48	53622

11	HNRPQ_HUMAN	Heterogeneous nuclear ribonucleoprotein Q	44	69788
12	DPYL2_HUMAN	Di-hydropyrimidinase-related protein 2	39	62711
13	NCRP1_HUMAN	Non-specific cytotoxic cell receptor protein 1 homolog	38	30942
14	ARGI1_HUMAN	Arginase-1	34	34884
15	AIFM1_HUMAN	Apoptosis-inducing factor 1, mitochondrial	34	67144
16	ANXA2_HUMAN	AnnexinA2	29	38808
17	PPCEL_HUMAN	Prolyl endopeptidase-like	24	84843
18	ZN830_HUMAN	Zinc finger protein 830	23	42144
19	GRP75_HUMAN	Stress-70 protein, mitochondrial	21	73920
20	LMNB1_HUMAN	Lamin-B1	21	66653
21	CC024_HUMAN	Uncharacterized protein C3orf24	21	20516
22	XRCC6_HUMAN	X-ray repair cross-complementing protein 6	21	70084
23	NUP85_HUMAN	Nuclear pore complex protein Nup85	20	75826
24	G3BP2_HUMAN	Ras GTPase-activating protein-binding protein 2	20	54145
25	EIF3J_HUMAN	Eukaryotic translation initiation factor 3 subunit J	20	29159
26	G3P_HUMAN	Glyceraldehyde-3-phosphate dehydrogenase	18	36201
27	RHG36_HUMAN	Rho GTPase-activating protein 36	18	61968
28	LRRN2_HUMAN	Leucine-rich repeat neuronal protein 2	16	79607
29	IAH1_HUMAN	Isoamyl acetate-hydrolyzing esterase 1 homolog	15	28037

30	OBSCN_HUMAN	Obscurin	14	9E+05
31	HERC1_HUMAN	Probable E3 ubiquitin-protein ligase HERC1	14	5E+05
Sample 3 (Expected MW = 37 kDa)				
prot_ hit_No	**prot_acccession**	**prot_description**	**prot_sc ore**	**prot_ Mass**
1	NPM_HUMAN	Nucleophosmin	56	32726
2	NCRP1_HUMAN	Non-specific cytotoxic cell receptor protein 1 homolog	51	30942
3	CAZA1_HUMAN	F-actin-capping protein subunit alpha-1	43	33073
4	THOC3_HUMAN	THO complex subunit 3	29	39431
5	ADPPT_HUMAN	L-aminoadipate-semialdehyde dehydrogenase-phosphopanteth einyl transferase	28	35981
6	IF2A_HUMAN	Eukaryotic translation initiation factor 2 subunit 1	27	36374
7	TOPK_HUMAN	Lymphokine-activated killer T-cell-originated protein kinase	26	36404
8	SRSF4_HUMAN	Serine/arginine-rich splicing factor 4	26	56759
9	SYNE2_HUMAN	Nesprin-2	21	8E+05
10	ROA2_HUMAN	Heterogeneous nuclear ribonucleoproteins A2/B1	21	37464
11	CCD87_HUMAN	Coiled-coil domain-containing protein 87	20	96741
12	KDM8_HUMAN	Lysine-specific demethylase 8	19	47867
13	HERC1_HUMAN	Probable E3 ubiquitin-protein ligase HERC1	19	5E+05
14	PTPRH_HUMAN	Receptor-type tyrosine-protein phosphatase H	18	1E+05

Sample 4 (Expected MW = 30 kDa)				
prot_ hit_No	**prot_acccession**	**prot_description**	**prot_sc ore**	**prot_ Mass**
1	RS3_HUMAN	40S ribosomal protein S3	85	26842
2	RS2_HUMAN	40S ribosomal protein S2	77	31590
3	RS3A_HUMAN	40S ribosomal protein S3a	48	30154
4	RL8_HUMAN	60S ribosomal protein L8	33	2 6035
5	LRMP_HUMAN	Lymphoid-restricted membrane protein	27	62767
6	CNGB3_HUMAN	Cyclic nucleotide-gated cation channel beta-3	26	92679
7	PHLB1_HUMAN	Pleckstrin homology-like domain family B member 1	23	2E+05
8	KDM8_HUMAN	Lysine-specific demethylase 8	22	47867
9	CCD87_HUMAN	Coiled-coil domain-containing protein 87	22	96741
10	S3TC1_HUMAN	SH3 domain and tetratricopeptide repeat-containing protein 1	20	1E+05
11	CCD96_HUMAN	Coiled-coil domain-containing protein 96	20	62958
12	TDRG1_HUMAN	Testis development-related protein 1	20	10636
13	MA1A1_HUMAN	Mannosyl-oligosaccharide 1,2-alpha-mannosidase IA	18	73150
14	ABL2_HUMAN	Abelson tyrosine-protein kinase 2	18	1E+05
15	H2B1A_HUMAN	Histone H2B type 1-A	17	14159
16	FANCJ_HUMAN	Fanconi anemia group J protein	17	1E+05
17	ADNP_HUMAN	Activity-dependent neuroprotector homeobox protein	16	1E+05

18	CHD2_HUMAN	Chromodomain-helicase-DNA-binding protein 2	16	2E+05
19	PLEC_HUMAN	Plectin	14	5E+05

* **prot_acccession**: Accession name in the database of UniProtKB/*Swiss-Prot.*

prot_score; The prot_score is derived from the ions scores. In Mascot, the ions score for an MS/MS match is based on the calculated probability, *P*, that the observed match between the experimental data and the database sequence is a random event.

Table 10. Homology of the LCE1 family proteins.

	LCE1A	LCE1B	LCE1C	LCE1D	LCE1E	LCE1F
LCE1A						
LCE1B	91					
LCE1C	95	96				
LCE1D	90	89	92			
LCE1E	95	93	96	93		
LCE1F	94	90	94	91	94	

Homology between the two of LCE1 family proteins (%) was calculated by clustalw2.

After qualify the specificity of PRMT5 antibody (Figure 13), I focused on PRMT5 for further analysis. This binding of LCE1F with PRMT5 was confirmed using an anti-PRMT5 specific antibody (Figure 13 and Figure 14A). As shown in Figure 14A, western blot analysis with anti-HA antibody corroborated the interaction between HA-LCE1F and PRMT5 in the precipitants.

To analyze the interaction between LCE1F and PRMT5, I performed immunoprecipitation with anti-PRMT5 antibody using extracts from the HEK293T cells transfected with HA-LCE1F. Western blot analysis of the precipitants revealed an interaction between endogenous PRMT5 and exogenous HA-tagged LCE1F (Figure 14*B*). Additionally, I co-transfected the cells with FLAG-PRMT5 and HA-LCE1F, and performed immunoprecipitation with an anti-HA antibody (Figure 14*C*) or an anti-FLAG antibody (Figure 14*D*). Subsequent western blot analysis clearly demonstrated an interaction between FLAG-tagged PRMT5 and HA-tagged LCE1F. These results imply that LCE1F interacts with PRMT5 in the cells.

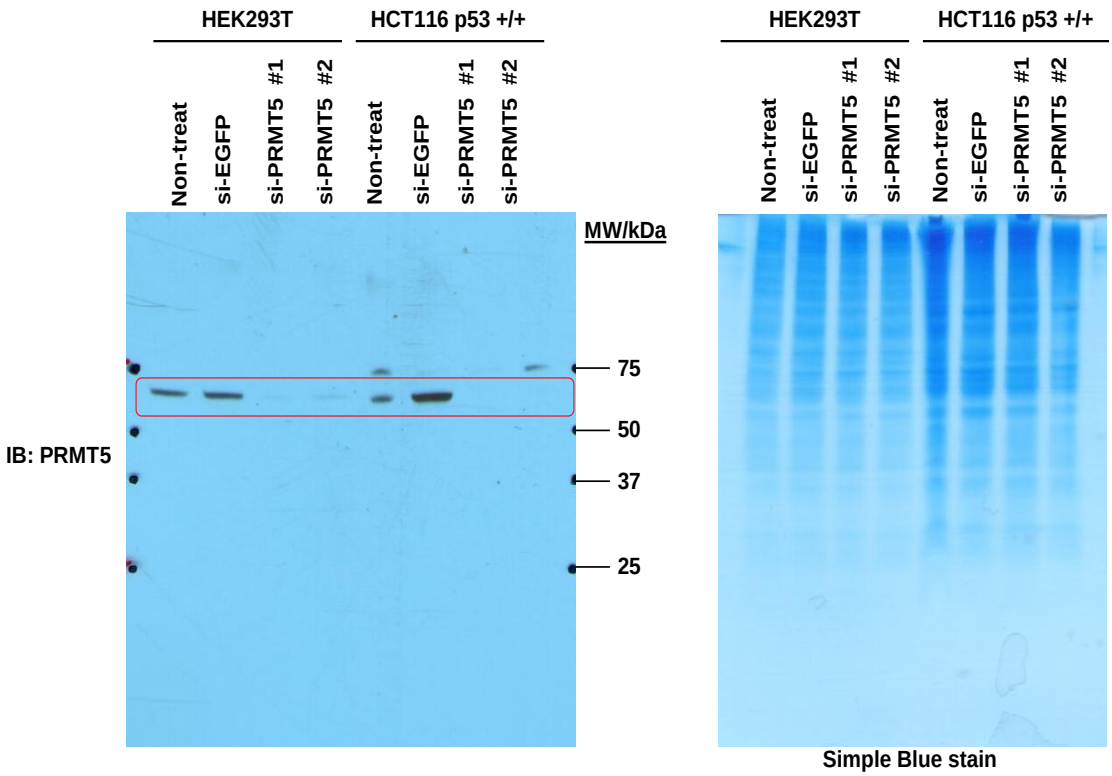

Figure 13. Knockdown of PRMT5 protein by two PRMT5-specific siRNA. Western blot analysis of PRMT5 protein with an anti-PRMT antibody (left panel). HEK293T and HCT116 $p53^{+/+}$ cells were treated with si-PRMT5s (#1 and #2) or control siRNA (si-EGFP), and proteins were extracted from the cells 60 h after transfection. The gel was stained with Simple Blue staining solution to visualize protein loading amount (right panel).

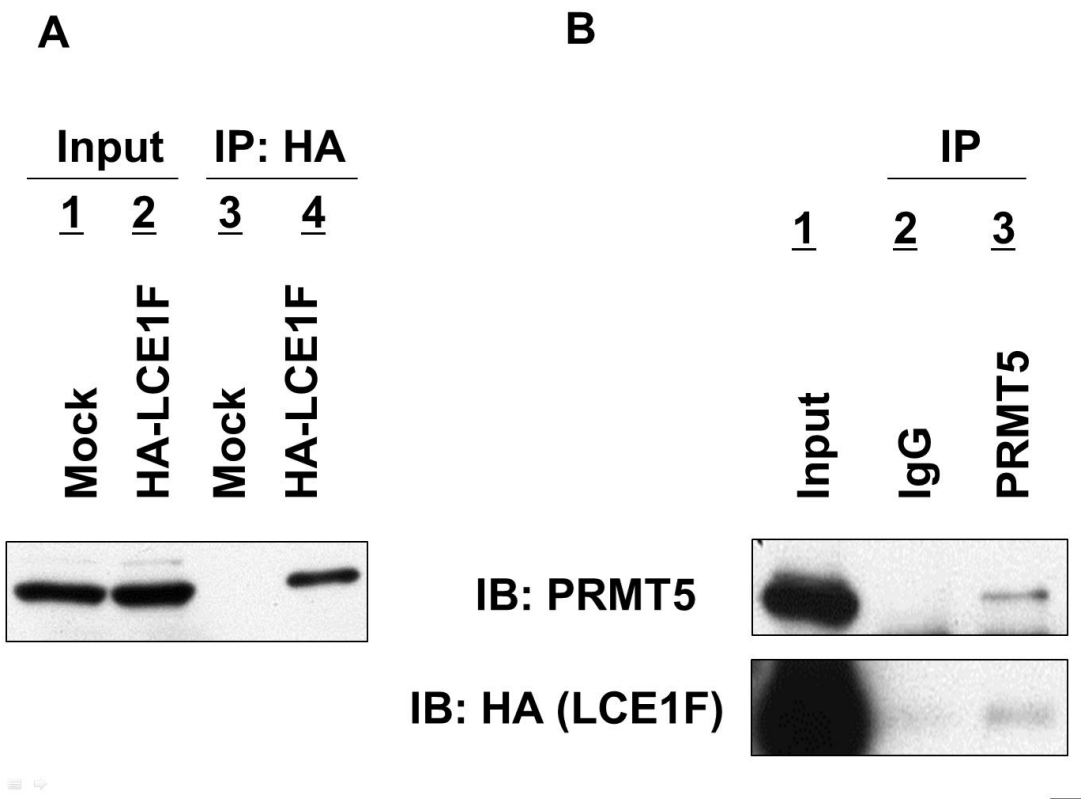
A
Input
IP: HA
1
2
3
4
Mock
HA-LCE1F
Mock
HA-LCE1F
B
IP
1
2
3
Input
IgG
PRMT5
IB: PRMT5
IB: HA (LCE1F)
C
Input
IP: HA
1
2
3
4
5
6
7
8
FLAG-Mock + - + - + - + -
FLAG-PRMT5 - + - + - + - +
HA-Mock + + - - + + - -
HA-LCE1F - - + + - - + +
IB: FLAG
IB: HA

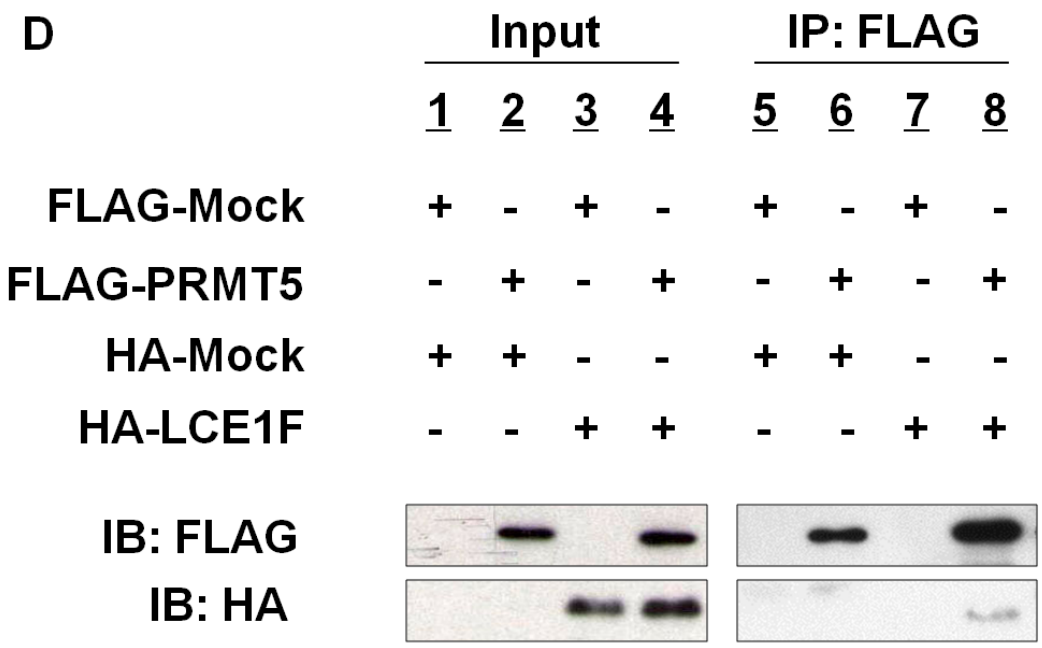

Figure 14. Interaction between HA-LCE1F and PRMT5 in cells. (A) Extracts from HEK293T cells transfected with either a Mock (empty) or plasmids expressing HA-LCE1F were used for western blot analysis with an anti-PRMT5 antibody. Proteins were immunoprecipitaed with anti-HA agarose (lanes 3 and 4). (B) Proteins were immunoprecipitated with an anti-PRMT5 antibody or normal rabbit IgG. Western blot analysis was performed with an anti-PRMT5 or anti-HA antibody. (C, D) Extracts from HEK293T cells transfected with indicated plasmids were used for western blot analysis. Proteins were immunoprecipitated with anti-HA agarose (C, lanes 5 - 8) or anti-FLAG antibody (D, lanes 5 - 8), and immunoblotted with anti-FLAG or anti-HA antibodies.

LCE1F Suppresses PRMT5 Activity

PRMT5 was reported to regulate the transcription of various genes through the methylation of arginine 8 on histone H3 (H3R8), which is considered to play an important role in human carcinogenesis [17, 19, 22, 24, 25]. Therefore, I investigated the biological significance of the interaction between PRMT5 and LCE1 members. Using anti-PRMT5 antibody (#07-405, Millipore), which had been reported to be available for immunocytochemistry by other researchers [34], immunocytochemical analysis revealed co-localization of LCE1F and PRMT5 in both the nucleus and the cytoplasm of the HCT116 $p53^{+/+}$ cells as shown in Figure 15. I then examined the methylation status of H3R8 by western blot with an antibody for symmetric di-methylation of H3R8 (H3R8me2s). In HCT116 $p53^{+/+}$ cells treated with Adriamycin, LCE1A, LCE1B, LCE1C, LCE1E and LCE1F were enhanced (Figure 8*D)*. Interestingly suppression of these LCE1 genes by siRNAs targeting these LCE1 genes significantly induced H3R8me2s compared with the control cells transfected with siEGFP (Figures 16*A* and *B)*. Consistent with this data, knockdown of p53 augmented the methylation level of H3R8me2s. To confirm this result, I transfected HEK293T cells with FLAG-PRMT5 with/without HA-LCE1F and investigated methylation levels of H3R8. As shown in Figure 16*C*, LCE1F significantly suppressed H3R8 methylation by

PRMT5. Taken together, my data implied that LCE1F may negatively regulate PRMT5-dependent H3R8 methylation.

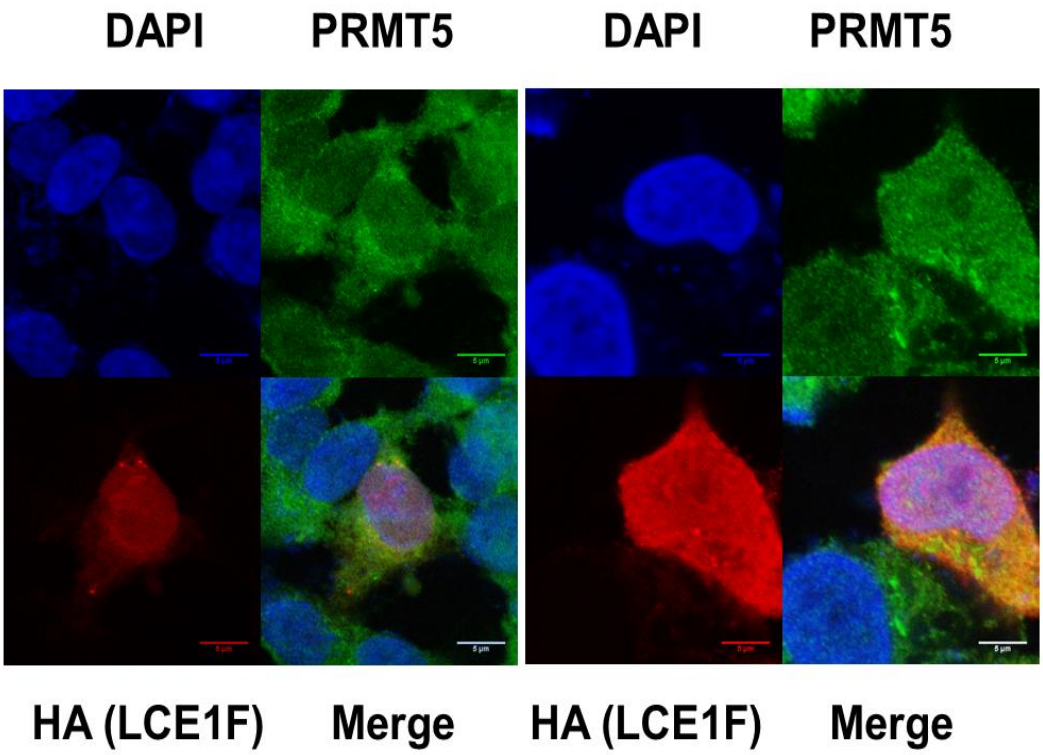

Figure 15. Co-localization of LCE1F and PRMT5. HCT116 $p53^{+/+}$ cells transfected with HA-LCE1F were fixed by 1.7% formaldehyde, stained with an anti-HA antibody (red) together with an anti-PRMT5 antibody (green) and visualized with secondary antibody. Nuclei were counter-stained with DAPI (Blue). Representative photos were shown. Scale bars, 5μm.

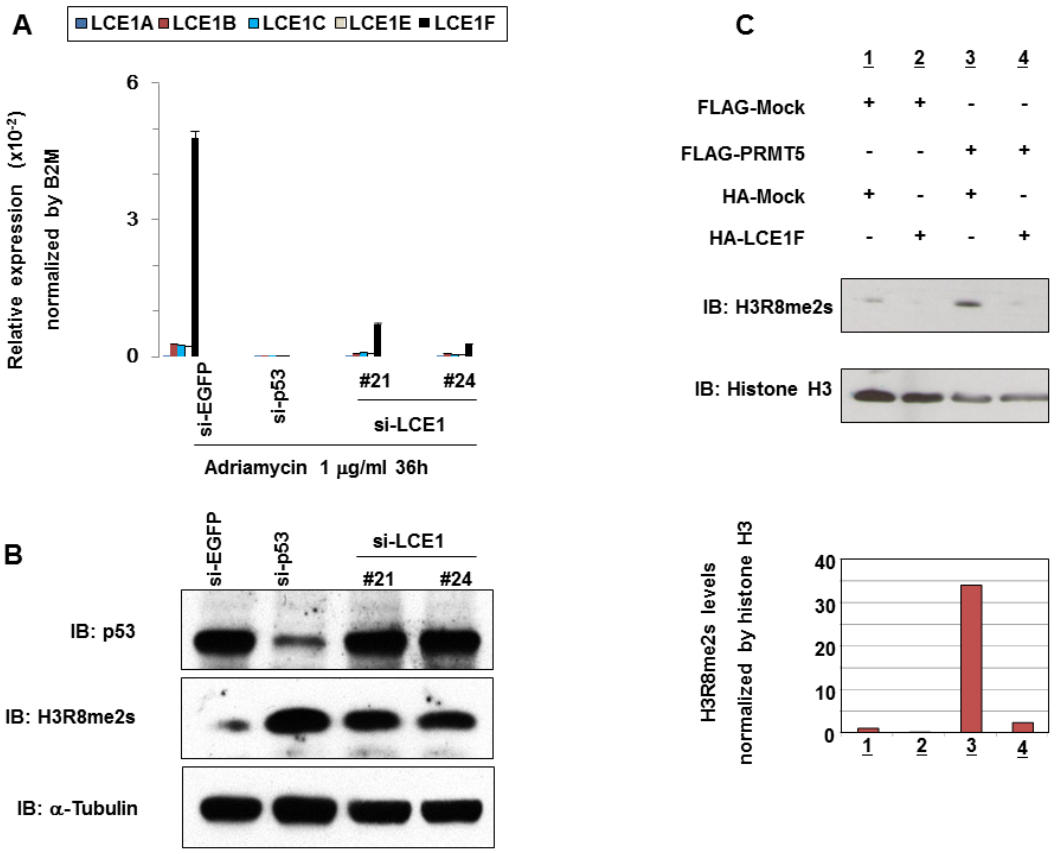

Figure 16. Effect of LCE1F on the symmetric di-methylation of H3R8. (A) Expression of *LCE1* genes was analyzed by real time qPCR analysis. HCT116 $p53^{+/+}$ cells were transfected with siRNAs targeting EGFP, p53 or LCE1. (B) Immunoblot analysis of p53 and symmetric di-methylated H3R8. (C) HEK293T cells expressing exogenous PRMT5 (lane 3 and 4) were co-transfected with/without HA-LCE1F. Data of western blot analysis with anti-H3R8 symmetric di-methyl arginine (H3R8me2s) or histone H3 (control) antibodies were quantified and shown in the histogram (lower panel).

Discussion

In this study, I found that the *LCE1* genes are novel p53-downstream genes and that the LCE1F protein interacts with the arginine methyltransferase PRMT5. Additionally our data suggested that LCE1F may suppress the methylation activity of PRMT5 at least on arginine 8 of histone H3 (Figure 16*C*) through the interaction with PRMT5, although the detailed mechanism is still elusive. PRMT5 is overexpressed in a wide range of human cancer, and plays a critical role in tumorigenesis through the regulation of histone methylation [17, 19, 22, 25-28]. Although I examined whether LCE1F expression may affect the expression of PRMT5, exogenous expression of LCE1F did not affect PRMT5 expression (Figure 17). Therefore deregulated LCE1F expression by the genetic alteration of p53 may be involved in carcinogenesis through the activation of PRMT5 without the change of PRMT5 expression in cancer cells.

The late cornified envelope (LCE) gene cluster contains multiple conserved genes encoding stratum-corneum proteins [9, 10, 13, 35]. My study demonstrated that most of the members in the LCE1 group are transcriptionally regulated by the tumor suppressor p53 although the induction levels varied. Concordantly, *LCE1* genes were reported to be significantly up-regulated in response to ultraviolet B (UVB) irradiation of the skin cells [9]. UV irradiation causes DNA damage, photoperoxidation of lipids, protein cross-linking, and isomerization of urocanic acid that lead to immunosuppression,

photo-induced ageing and cancer. p53 protein acts as a molecular sensor for the damages generated by UV irradiation through mediating cell cycle arrest and apoptosis in damaged keratinocytes [36-40]. Taken together, cells may possess the function to express *LCE1* family genes through p53 activation in order to eliminate dangerous cells with DNA damages. Importantly, LCE1 family proteins show a high level of sequence similarity and LCE1F has more than 90% homology with other members (LCE1A-E, Table 10). Since the expression of *LCE1* cluster genes is regulated by p53 as a whole (may not be all of the members), this protein family members might play important roles to complementally or redundantly function as a tumor suppressor.

I identified PRMT5, a histone methyltransferase, as a key binding partner of LCE1F. Current progress of molecular medicine revealed that the enzymes relevant to histone methylation play critical roles in human carcinogenesis [33, 41-51]. PRMT5 is one of the type II arginine methyltransferases, which catalyze the formation of sDMA and regulates various cellular pathways by targeting many histone and non-histone proteins including p53 [19, 20, 22, 25, 52]. A number of reports described the importance of this arginine methyltransferase in tumorigenesis [17, 19, 21, 22, 25, 52-56]. Intriguingly, PRMT5 was reported to interact with Brahma-related gene 1 (BRG1) - and human Brahma (hBRM) -based hSWI/SNF chromatin remodelers and methylate arginine 8 on

histone H3 [24]. The H3R8 methylation medicated by PRMT5-containing BRG1 and hBRM complexes directly repressed the expression of tumor suppressor genes such as Retinoblastoma (RB) family proteins [24, 53]. In particular, the knockdown of PRMT5 could induce the cell death by reactivate RB pathway, which is suppressed in many cancers [53, 57]. This line of pathway seems to be a key mechanism in the PRMT5-dependent tumorigenesis. My data presented here have implied that LCE1F, which is regulated by the tumor suppressor p53, negatively regulates H3R8 methylation mediated by PRMT5 (Figures 15*A* and 15*B*). Therefore, inactivation of p53 may be essential for the constitutive activation of PRMT5 that represses RB family proteins. This possibility is interesting to investigate in my future studies.

In conclusion, in this study I found new p53-downstream genes, *LCE1* cluster genes, and elucidated a new role of p53, which is down-regulation of PRMT5 through the binding with LCE1F (Figure 18). Notably, PRMT5 was reported to methylate p53 through the direct interaction and this methylation prevents p53-dependent apoptosis in cancer cells [52]. Taking together, LCE1F may play a role in accelerating p53-dependent apoptosis through the suppression of PRMT5. Further functional analysis may explore the importance of the LCE1 group proteins as tumor suppressors and the physiological relevance among p53 downstream genes.

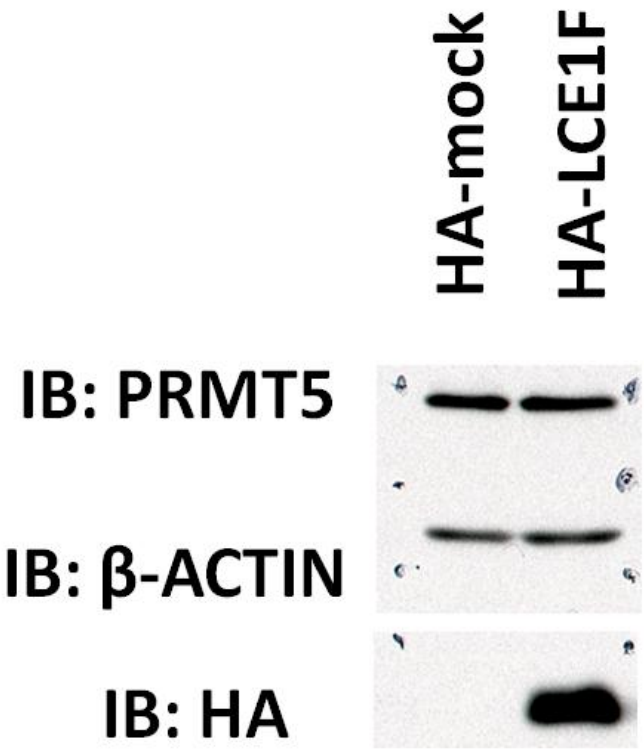

Figure 17. Stability of PRMT5 in response to overexpression of LCE1F. Expression of PRMT5 protein in response to the overexpression of LCE1F. Western blot analysis was carried out using lysates from HEK293T cells transfected with HA-tagged LCE1F. Immunoblot analysis with anti-HA, anti-PRMT5, or anti-β-actin antibodies.

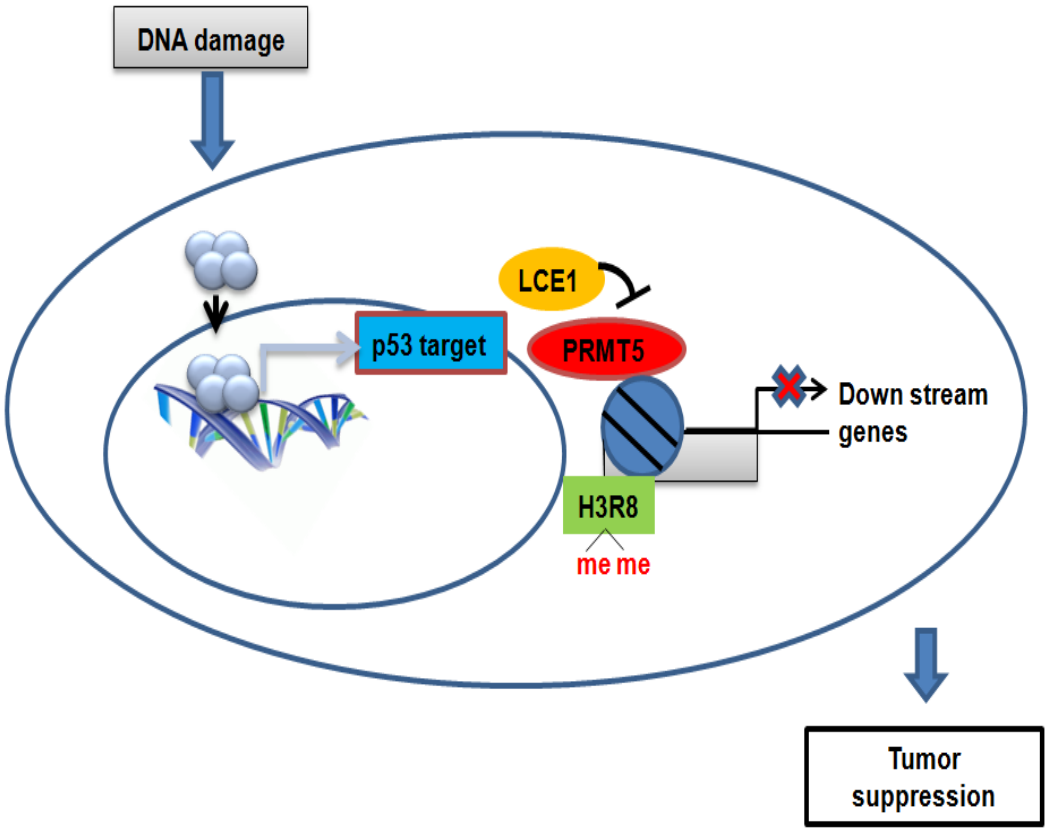

Figure 18. Negative regulation of PRMT5 activity through the p53-dependent LCE1 induction. A model of p53-dependent regulation of PRMT5 methyltransferase activity through LCE1 family members.

References

[1] T. Soussi, "TP53 mutations in human cancer: database reassessment and prospects for the next decade," *Adv Cancer Res,* vol. 110, pp. 107-39, 2011.

[2] B. Leroy, J. L. Fournier, C. Ishioka, P. Monti, A. Inga, G. Fronza, *et al.*, "The TP53 website: an integrative resource centre for the TP53 mutation database and TP53 mutant analysis," *Nucleic Acids Res,* vol. 41, pp. D962-9, Jan 2013.

[3] R. Beckerman and C. Prives, "Transcriptional regulation by p53," *Cold Spring Harb Perspect Biol,* vol. 2, p. a000935, Aug 2010.

[4] K. Oda, H. Arakawa, T. Tanaka, K. Matsuda, C. Tanikawa, T. Mori, *et al.*, "p53AIP1, a potential mediator of p53-dependent apoptosis, and its regulation by Ser-46-phosphorylated p53.," *Cell,* vol. 102, pp. 849-62, Sep 2000.

[5] H. Tanaka, H. Arakawa, T. Yamaguchi, K. Shiraishi, S. Fukuda, K. Matsui, *et al.*, "A ribonucleotide reductase gene involved in a p53-dependent cell-cycle checkpoint for DNA damage," *Nature,* vol. 404, pp. 42-9, Mar 2 2000.

[6] C. Tanikawa, K. Matsuda, S. Fukuda, Y. Nakamura, and H. Arakawa, "p53RDL1 regulates p53-dependent apoptosis," *Nat Cell Biol,* vol. 5, pp. 216-23, Mar 2003.

[7] Y. Nakamura, "Isolation of p53-target genes and their functional analysis," *Cancer Sci,* vol. 95, pp. 7-11, Jan 2004.

[8] C. Tanikawa, Y. Furukawa, N. Yoshida, H. Arakawa, Y. Nakamura, and K. Matsuda, "XEDAR as a putative colorectal tumor suppressor that mediates p53-regulated anoikis pathway.," *Oncogene,* vol. 28, pp. 3081-92, Aug 2009.

[9] B. Jackson, C. M. Tilli, M. J. Hardman, A. A. Avilion, M. C. MacLeod, G. S. Ashcroft, *et al.*, "Late cornified envelope family in differentiating epithelia--response to calcium and ultraviolet irradiation," *J Invest Dermatol,* vol. 124, pp. 1062-70, May 2005.

[10] D. Marshall, M. J. Hardman, K. M. Nield, and C. Byrne, "Differentially expressed late constituents of the epidermal cornified envelope," *Proc Natl Acad Sci U S A,* vol. 98, pp. 13031-6, Nov 6 2001.

[11] E. Candi, R. Schmidt, and G. Melino, "The cornified envelope: a model of cell death in the skin," *Nat Rev Mol Cell Biol,* vol. 6, pp. 328-40, Apr 2005.

[12] D. Mischke, B. P. Korge, I. Marenholz, A. Volz, and A. Ziegler, "Genes encoding structural proteins of epidermal cornification and S100 calcium-binding proteins form a gene complex ("epidermal differentiation complex") on human chromosome 1q21," *J Invest Dermatol,* vol. 106, pp. 989-92, May 1996.

[13] J. G. Bergboer, G. S. Tjabringa, M. Kamsteeg, I. M. van Vlijmen-Willems, D. Rodijk-Olthuis, P. A. Jansen, *et al.*, "Psoriasis risk genes of the late cornified

envelope-3 group are distinctly expressed compared with genes of other LCE groups," *Am J Pathol,* vol. 178, pp. 1470-7, Apr 2011.

[14] X. P. Zhao and J. T. Elder, "Positional cloning of novel skin-specific genes from the human epidermal differentiation complex," *Genomics,* vol. 45, pp. 250-8, Oct 15 1997.

[15] S. J. Brown, C. M. Tilli, B. Jackson, A. A. Avilion, M. C. MacLeod, L. J. Maltais, *et al.*, "Rodent Lce gene clusters; new nomenclature, gene organization, and divergence of human and rodent genes," *J Invest Dermatol,* vol. 127, pp. 1782-6, Jul 2007.

[16] M. T. Bedford and S. G. Clarke, "Protein arginine methylation in mammals: who, what, and why," *Mol Cell,* vol. 33, pp. 1-13, Jan 16 2009.

[17] Y. Yang and M. T. Bedford, "Protein arginine methyltransferases and cancer," *Nat Rev Cancer,* vol. 13, pp. 37-50, Jan 2013.

[18] S. Gkountela, Z. Li, C. J. Chin, S. A. Lee, and A. T. Clark, "PRMT5 is Required for Human Embryonic Stem Cell Proliferation But Not Pluripotency," *Stem Cell Rev,* vol. 10, pp. 230-9, Apr 2014.

[19] C. Nicholas, J. Yang, S. B. Peters, M. A. Bill, R. A. Baiocchi, F. Yan, *et al.*, "PRMT5 is upregulated in malignant and metastatic melanoma and regulates

expression of MITF and p27(Kip1.)," *PLoS One,* vol. 8, p. e74710, 2013.

[20] M. A. Powers, M. M. Fay, R. E. Factor, A. L. Welm, and K. S. Ullman, "Protein arginine methyltransferase 5 accelerates tumor growth by arginine methylation of the tumor suppressor programmed cell death 4," *Cancer Res,* vol. 71, pp. 5579-87, Aug 15 2011.

[21] X. Bao, S. Zhao, T. Liu, Y. Liu, Y. Liu, and X. Yang, "Overexpression of PRMT5 promotes tumor cell growth and is associated with poor disease prognosis in epithelial ovarian cancer," *J Histochem Cytochem,* vol. 61, pp. 206-17, Mar 2013.

[22] V. Karkhanis, Y. J. Hu, R. A. Baiocchi, A. N. Imbalzano, and S. Sif, "Versatility of PRMT5-induced methylation in growth control and development," *Trends Biochem Sci,* vol. 36, pp. 633-41, Dec 2011.

[23] S. Majumder, L. Alinari, S. Roy, T. Miller, J. Datta, S. Sif, *et al.*, "Methylation of histone H3 and H4 by PRMT5 regulates ribosomal RNA gene transcription," *J Cell Biochem,* vol. 109, pp. 553-63, Feb 15 2010.

[24] S. Pal, S. N. Vishwanath, H. Erdjument-Bromage, P. Tempst, and S. Sif, "Human SWI/SNF-associated PRMT5 methylates histone H3 arginine 8 and negatively regulates expression of ST7 and NM23 tumor suppressor genes," *Mol Cell Biol,*

vol. 24, pp. 9630-45, Nov 2004.

[25] S. Pal, R. A. Baiocchi, J. C. Byrd, M. R. Grever, S. T. Jacob, and S. Sif, "Low levels of miR-92b/96 induce PRMT5 translation and H3R8/H4R3 methylation in mantle cell lymphoma," *EMBO J*, vol. 26, pp. 3558-69, Aug 8 2007.

[26] Z. Gu, S. Gao, F. Zhang, Z. Wang, W. Ma, R. E. Davis, *et al.*, "Protein arginine methyltransferase 5 is essential for growth of lung cancer cells," *Biochem J*, vol. 446, pp. 235-41, Sep 1 2012.

[27] Z. Gu, Y. Li, P. Lee, T. Liu, C. Wan, and Z. Wang, "Protein arginine methyltransferase 5 functions in opposite ways in the cytoplasm and nucleus of prostate cancer cells," *PLoS One*, vol. 7, p. e44033, 2012.

[28] F. Yan, L. Alinari, M. E. Lustberg, L. K. Martin, H. M. Cordero-Nieves, Y. Banasavadi-Siddegowda, *et al.*, "Genetic validation of the protein arginine methyltransferase PRMT5 as a candidate therapeutic target in glioblastoma," *Cancer Res*, vol. 74, pp. 1752-65, Mar 2014.

[29] C. Tanikawa, H. Nakagawa, Y. Furukawa, Y. Nakamura, and K. Matsuda, "CLCA2 as a p53-inducible senescence mediator," *Neoplasia*, vol. 14, pp. 141-9, Feb 2012.

[30] R. Hamamoto, Y. Furukawa, M. Morita, Y. Iimura, F. P. Silva, M. Li, *et al.*,

"SMYD3 encodes a histone methyltransferase involved in the proliferation of cancer cells," *Nat Cell Biol,* vol. 6, pp. 731-40, Aug 2004.

[31] R. Hamamoto, F. P. Silva, M. Tsuge, T. Nishidate, T. Katagiri, Y. Nakamura, *et al.*, "Enhanced SMYD3 expression is essential for the growth of breast cancer cells," *Cancer Sci,* vol. 97, pp. 113-8, Feb 2006.

[32] L. Piao, H. Nakagawa, K. Ueda, S. Chung, K. Kashiwaya, H. Eguchi, *et al.*, "C12orf48, termed PARP-1 binding protein, enhances poly(ADP-ribose) polymerase-1 (PARP-1) activity and protects pancreatic cancer cells from DNA damage," *Genes Chromosomes Cancer,* vol. 50, pp. 13-24, Jan 2011.

[33] M. Kogure, M. Takawa, V. Saloura, K. Sone, L. Piao, K. Ueda, *et al.*, "The oncogenic polycomb histone methyltransferase EZH2 methylates lysine 120 on histone H2B and competes ubiquitination," *Neoplasia,* vol. 15, pp. 1251-61, Nov 2013.

[34] Z. Li, J. Yu, L. Hosohama, K. Nee, S. Gkountela, S. Chaudhari, *et al.*, "The Sm protein methyltransferase PRMT5 is not required for primordial germ cell specification in mice," *EMBO J,* Dec 2014.

[35] L. Tong, R. M. Corrales, Z. Chen, A. L. Villarreal, C. S. De Paiva, R. Beuerman, *et al.*, "Expression and regulation of cornified envelope proteins in human

corneal epithelium," *Invest Ophthalmol Vis Sci*, vol. 47, pp. 1938-46, May 2006.

[36] C. L. Benjamin, S. E. Ullrich, M. L. Kripke, and H. N. Ananthaswamy, "p53 tumor suppressor gene: a critical molecular target for UV induction and prevention of skin cancer," *Photochem Photobiol*, vol. 84, pp. 55-62, Jan-Feb 2008.

[37] A. Ziegler, A. S. Jonason, D. J. Leffell, J. A. Simon, H. W. Sharma, J. Kimmelman, *et al.*, "Sunburn and p53 in the onset of skin cancer," *Nature*, vol. 372, pp. 773-6, Dec 22-29 1994.

[38] M. Yamaizumi and T. Sugano, "U.v.-induced nuclear accumulation of p53 is evoked through DNA damage of actively transcribed genes independent of the cell cycle," *Oncogene*, vol. 9, pp. 2775-84, Oct 1994.

[39] C. N. Gujuluva, J. H. Baek, K. H. Shin, H. M. Cherrick, and N. H. Park, "Effect of UV-irradiation on cell cycle, viability and the expression of p53, gadd153 and gadd45 genes in normal and HPV-immortalized human oral keratinocytes," *Oncogene*, vol. 9, pp. 1819-27, Jul 1994.

[40] W. Maltzman and L. Czyzyk, "UV irradiation stimulates levels of p53 cellular tumor antigen in nontransformed mouse cells," *Mol Cell Biol*, vol. 4, pp. 1689-94, Sep 1984.

[41] H. S. Cho, T. Shimazu, G. Toyokawa, Y. Daigo, Y. Maehara, S. Hayami, *et al.*, "Enhanced HSP70 lysine methylation promotes proliferation of cancer cells through activation of Aurora kinase B," *Nat Commun,* vol. 3, p. 1072, 2012.

[42] S. Hayami, J. D. Kelly, H. S. Cho, M. Yoshimatsu, M. Unoki, T. Tsunoda, *et al.*, "Overexpression of LSD1 contributes to human carcinogenesis through chromatin regulation in various cancers," *Int J Cancer,* vol. 128, pp. 574-86, Feb 1 2011.

[43] S. Hayami, M. Yoshimatsu, A. Veerakumarasivam, M. Unoki, Y. Iwai, T. Tsunoda, *et al.*, "Overexpression of the JmjC histone demethylase KDM5B in human carcinogenesis: involvement in the proliferation of cancer cells through the E2F/RB pathway," *Mol Cancer,* vol. 9, p. 59, Mar 13 2010.

[44] M. Takawa, K. Masuda, M. Kunizaki, Y. Daigo, K. Takagi, Y. Iwai, *et al.*, "Validation of the histone methyltransferase EZH2 as a therapeutic target for various types of human cancer and as a prognostic marker," *Cancer Sci,* vol. 102, pp. 1298-1305, Jul 2011.

[45] G. Toyokawa, H. S. Cho, K. Masuda, Y. Yamane, M. Yoshimatsu, S. Hayami, *et al.*, "Histone Lysine Methyltransferase Wolf-Hirschhorn Syndrome Candidate 1 Is Involved in Human Carcinogenesis through Regulation of the Wnt Pathway,"

Neoplasia, vol. 13, pp. 887-98, Oct 2011.

[46] M. Yoshimatsu, G. Toyokawa, S. Hayami, M. Unoki, T. Tsunoda, H. I. Field, *et al.*, "Dysregulation of PRMT1 and PRMT6, Type I arginine methyltransferases, is involved in various types of human cancers," *Int J Cancer,* vol. 128, pp. 562-73, Feb 1 2011.

[47] M. Takawa, H. S. Cho, S. Hayami, G. Toyokawa, M. Kogure, Y. Yamane, *et al.*, "Histone Lysine Methyltransferase SETD8 Promotes Carcinogenesis by Deregulating PCNA Expression," *Cancer Res,* vol. 72, pp. 3217-3227, Jul 1 2012.

[48] H. S. Cho, J. D. Kelly, S. Hayami, G. Toyokawa, M. Takawa, M. Yoshimatsu, *et al.*, "Enhanced expression of EHMT2 is involved in the proliferation of cancer cells through negative regulation of SIAH1," *Neoplasia,* vol. 13, pp. 676-84, 2011.

[49] H. S. Cho, G. Toyokawa, Y. Daigo, S. Hayami, K. Masuda, N. Ikawa, *et al.*, "The JmjC domain-containing histone demethylase KDM3A is a positive regulator of the G1/S transition in cancer cells via transcriptional regulation of the HOXA1 gene," *Int J Cancer,* vol. 131, pp. E179-89, Aug 1 2012.

[50] G. Toyokawa, H. S. Cho, Y. Iwai, M. Yoshimatsu, M. Takawa, S. Hayami, *et al.*,

"The histone demethylase JMJD2B plays an essential role in human carcinogenesis through positive regulation of cyclin-dependent kinase 6," *Cancer Prev Res (Phila),* vol. 4, pp. 2051-61, Dec 2011.

[51] M. Kogure, M. Takawa, H. S. Cho, G. Toyokawa, K. Hayashi, T. Tsunoda, *et al.*, "Deregulation of the histone demethylase JMJD2A is involved in human carcinogenesis through regulation of the G/S transition," *Cancer Lett,* Apr 18 2013.

[52] M. Jansson, S. T. Durant, E. C. Cho, S. Sheahan, M. Edelmann, B. Kessler, *et al.*, "Arginine methylation regulates the p53 response," *Nat Cell Biol,* vol. 10, pp. 1431-9, Dec 2008.

[53] L. Wang, S. Pal, and S. Sif, "Protein arginine methyltransferase 5 suppresses the transcription of the RB family of tumor suppressors in leukemia and lymphoma cells," *Mol Cell Biol,* vol. 28, pp. 6262-77, Oct 2008.

[54] E. C. Cho, S. Zheng, S. Munro, G. Liu, S. M. Carr, J. Moehlenbrink, *et al.*, "Arginine methylation controls growth regulation by E2F-1," *EMBO J,* vol. 31, pp. 1785-97, Apr 4 2012.

[55] F. Yan, L. Alinari, M. E. Lustberg, L. Katherine Martin, H. M. Cordero-Nieves, Y. Banasavadi-Siddegowda, *et al.*, "Genetic Validation of the Protein Arginine

Methyltransferase PRMT5 as a Candidate Therapeutic Target in Glioblastoma," *Cancer Res*, vol. 74, pp. 1752-65, Mar 15 2014.

[56] K. Shilo, X. Wu, S. Sharma, M. Welliver, W. Duan, M. Villalona-Calero, *et al.*, "Cellular localization of protein arginine methyltransferase-5 correlates with grade of lung tumors," *Diagn Pathol*, vol. 8, p. 201, 2013.

[57] J. Chung, V. Karkhanis, S. Tae, F. Yan, P. Smith, L. W. Ayers, *et al.*, "Protein arginine methyltransferase 5 (PRMT5) inhibition induces lymphoma cell death through reactivation of the retinoblastoma tumor suppressor pathway and polycomb repressor complex 2 (PRC2) silencing," *J Biol Chem*, vol. 288, pp. 35534-47, Dec 2013.

Disclosure of Conflicts of Interest

I do not have any conflicts of interest to disclose. This study was supported by Project for Development of Innovation Research on Cancer Therapeutics and partly by research grants from Oncotherapy Science.

Acknowledgements

I would like to thank a lot of people for their support, encouragement and guidance during my four and half years of research and study in the University of Tokyo.

First and foremost, I would like to express my deepest and sincerest gratitude to my supervisor, Professor Yusuke Nakamura, for the continuous support, for his patience, motivation, immense knowledge and enthusiasm to cure cancer. I could not have imagined having a better advisor and mentor for my PhD study and research. I could not believe such a talented scientist spending so much time on educating young researchers. It is impossible for me to make any efforts without his support, especially offering me to continue this project in the University of Chicago for one year.

Next, I would like to thank deeply and sincerely to my supervisor, Professor Yoichi Furukawa. His critical comments and gentle guidance helped me a lot all the time, especially writing of this thesis and applying of the scholarship. I would never have been able to finish my dissertation without his great guidance and assistance. Every time it is really beneficial and enjoyable for me to talk with such a strict and nice supervisor. I will keep all his instructions in my mind.

Besides my advisors, I would like to appreciate all of my thesis committee: Professor Nobuaki Yoshida, Professor Yuji Yamanashi, Professor Naohide Yamashita, Associate Professor Takeshi Sasaki and Associate Professor Naoya Kato, for their encouragement, insightful comments, and hard questions.

My sincere thanks also go to Drs. Koichi Matsuda and Chizu Tanikawa for their super support and strict training from the very beginning of my research. In particular, I am grateful to Dr. Chizu Tanikawa for enlightening me the first taste of research. I believe that there will be no difficulty I cannot overcome in the future even here I can survive.

I would like to thank Dr. Ryuji Hamamoto for mental education and close cooperation during my study in the University of Chicago. His great mentorship and tremendous trust enable me to get through the forest. It will live in my heart forever.

It is really nice of my good friends Drs. Jiaying Lin, Takashi Fujitomo, Yuki Funauchi, Lianhua Piao and Paulisally Hau Yi Lo to stand with me and share their brilliant ideas and technical supports.

Meanwhile, I would like to thank Dr. Koji Ueda for the mass spectrometric analysis and wonderful discussions.

I would like to appreciate all members of the Laboratory of Molecular Medicine, Human Genome Center, Institute of Medical Science, the University of Tokyo as well as all labmates from the University of Chicago for their constructive comments and warm encouragement. It is so nice to work with my brilliant colleagues.

I would like to thank all people who help me, teach me, care me and love me, as well as expressing my apology that I could not mention them personally one by one.

Last but not the least, I would like to thank my family, particularly my wife and son. They have always been supportive, understanding and encouraging all the time through my study abroad. I dedicate this thesis to them.

Publication

The content of this manuscript was published with the title of Late Cornified Envelope Group I, a Novel Target of p53, Regulates PRMT5 Activity in *Neoplasia* 2014 Aug;16 (8): 656-64. doi: 10.1016/j.neo.2014.07.008.